TU Delft

Delft University of Technology

Modeling the fate of viruses in aquifers

multi-kinetics reactive transport, risk assessment, and governing parameters

Rafini, Silvain; Chesnaux, Romain; Lompe, Kim Maren; Barbeau, Benoit; Claveau-Mallet, Dominique ; Richard, Dominique

DOI
10.1016/j.scitotenv.2023.166276

Publication date
2023

Document Version
Final published version

Published in
Science of the Total Environment

Citation (APA)
Rafini, S., Chesnaux, R., Lompe, K. M., Barbeau, B., Claveau-Mallet, D., & Richard, D. (2023). Modeling the fate of viruses in aquifers: multi-kinetics reactive transport, risk assessment, and governing parameters. *Science of the Total Environment*, *903*, Article 166276. https://doi.org/10.1016/j.scitotenv.2023.166276

Important note
To cite this publication, please use the final published version (if applicable).
Please check the document version above.

Copyright
Other than for strictly personal use, it is not permitted to download, forward or distribute the text or part of it, without the consent of the author(s) and/or copyright holder(s), unless the work is under an open content license such as Creative Commons.

Takedown policy
Please contact us and provide details if you believe this document breaches copyrights.
We will remove access to the work immediately and investigate your claim.

This work is downloaded from Delft University of Technology.
For technical reasons the number of authors shown on this cover page is limited to a maximum of 10.

Green Open Access added to TU Delft Institutional Repository

'You share, we take care!' - Taverne project

https://www.openaccess.nl/en/you-share-we-take-care

Otherwise as indicated in the copyright section: the publisher is the copyright holder of this work and the author uses the Dutch legislation to make this work public.

Science of the Total Environment 903 (2023) 166276

Contents lists available at ScienceDirect

Science of the Total Environment

journal homepage: www.elsevier.com/locate/scitotenv

Modeling the fate of viruses in aquifers: Multi-kinetics reactive transport, risk assessment, and governing parameters

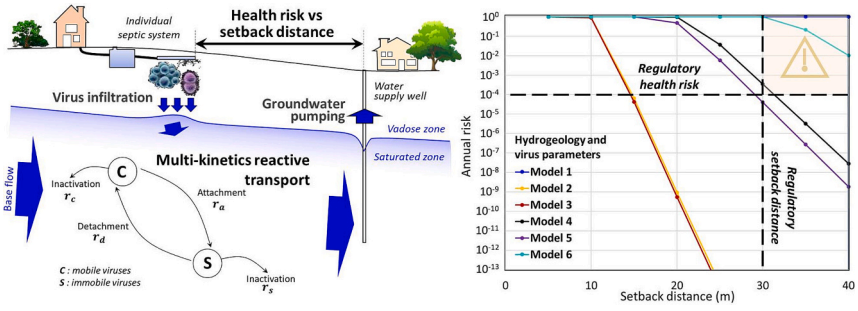
Silvain Rafini [a], Romain Chesnaux [a,*], Kim Maren Lompe [b], Benoit Barbeau [c], Dominique Claveau-Mallet [c], Dominique Richard [a]

[a] Groupe de Recherche Risque Ressource Eau » (R2Eau), Université du Québec à Chicoutimi, Département des sciences appliquées, Qc, Canada
[b] Water Management, Civil Engineering and Geoscience, Delft University of Technology, the Netherlands
[c] Polytechnique Montréal, Département des génies civil, géologique et mines, Qc, Canada

HIGHLIGHTS

- Numerical simulations for the transport of viruses in aquifers are performed.
- The risk is assessed by setback distances between septic systems and pumping wells.
- The hydraulic and kinetic parameters mostly control the fate of viruses.
- A maximum of 10^{-4} infections/person/year and a 30 m setback distance is targeted.

GRAPHICAL ABSTRACT



ARTICLE INFO

Editor: Daniel Alessi

Keywords:
Transport of viruses
Aquifers
Septic system
Pumping well
Setback distance
Multi-kinetics reactive transport

ABSTRACT

The transport of viruses in groundwater is a complex process controlled by both hydrodynamic and reaction parameters. Characterizing the transport of viruses in groundwater is of crucial importance for investigating health risks associated with groundwater consumption from private individual or residential pumping wells. Setback distances between septic systems, which are the source of viruses, and pumping wells must be designed to offer sufficient groundwater travel times to allow the viral load to degrade sufficiently to be acceptable for community health needs. This study consists of developing numerical simulations for the reactive transport of viruses in the subsurface. These simulations are validated using published results of laboratory and field experiments on virus transport in the subsurface and applying previously developed analytical solutions. The numerical model is then exploited to investigate the sensitivity of the fate of viruses in saturated porous media to hydraulic parameters and the coefficients of kinetic reactions. This sensitivity analysis provides valuable insights into the prevailing factors governing health risks caused by contaminated water in private wells in rural residential contexts. The simulations of virus transport are converted into health risk predictions through dose–response relationships. Risk predictions for a wide range of input parameters are compared with the international regulatory health risk target of a maximum of 10^{-4} infections/person/year and a 30 m setback distance to identify critical subsurface contexts that should be the focus of regulators.

* Corresponding author.
E-mail address: rchesnau@uqac.ca (R. Chesnaux).

https://doi.org/10.1016/j.scitotenv.2023.166276
Received 8 April 2023; Received in revised form 23 July 2023; Accepted 11 August 2023
Available online 19 August 2023
0048-9697/© 2023 Elsevier B.V. All rights reserved.

1. Introduction

Groundwater is a vital resource in many regions where surficial water is either lacking or unexploitable. Groundwater accounts for 30 % of the world's freshwater, nearly half of the global annual demand for drinking water (Khare et al., 2017), one-fifth of the annual global water consumption (Hiscock, 2011), and daily water use for an estimated two billion people (Hiscock, 2011; Murphy et al., 2017). The supply of safe drinking water in rural settings lacking collective distribution networks almost entirely depends on groundwater. For instance, 90 % of the rural domestic demand in the United States is provided by groundwater (Barber, 2009). Across Canada, about four million (12 %) people are served by private groundwater supply, mostly in rural areas. In the province of Quebec, Canada, groundwater resources supply water to 25 % of the population (MELCC, 2023), among which 70 %, or 1.2 million people (14 % of the total population), use individual private wells for their water supply (Féret, 2016).

In rural contexts, where collective water and sewage networks are not implemented because of the great distances between residences, wastewater must be managed on a site-specific basis using autonomous on-site solutions. Individual septic systems (ISS) have issues related to the infiltration of clarified wastewater into the soil. They are hence a significant source of contaminants, e.g., nutrient and pathogen leaks into aquifers. Viral concentrations of up to 10^9 viruses/L have been measured below conventional septic systems (Anderson and Weber, 2004; Blaschke et al., 2016). Under optimal operation conditions (i.e., correctly designed, installed, and maintained septic systems), viral removal in ISS is about 4 log (Lusk et al., 2017; Adegoke and Stenstrom, 2019; Eregno and Heistad, 2019; Blaschke et al., 2016). Additional removal of viruses subsequently occurs via natural attenuation mechanisms during subsurface transport through the aquifer. Residential housing developments are expanding into rural areas surrounding major urban centers; however, the urbanization of these peri-urban zones is occurring before the implementation of centralized wastewater collection and drinking water supply. The accompanying densification of septic systems puts local aquifers and individual drinking water wells under pressure from viral and nutrient contamination (Bremer and Harter, 2012).

The quality of drinking water in private wells remains a global public health concern (Powell et al., 2003; Bradbury et al., 2013; Trimper, 2010; Borchardt et al., 2012; Gunnarsdottir et al., 2013). A review by Schuster et al. (2005) revealed that between 1974 and 2001, two-thirds of waterborne infectious disease outbreaks in Canada occurred in groundwater supplied by private or semi-private contaminated wells. Murphy et al. (2016, 2017) estimated that contaminated drinking water from untreated private wells produces approximately 110,700 annual cases of acute gastroenteritis in Canada (0.027/person/year). This incidence rate decreases to 0.016/person/year for the Canadian population supplied by small, chlorinated water-supply systems. By crudely applying these rates to the global groundwater-reliant population (2.2 billion), Murphy et al. (2017) derived that the annual occurrence of groundwater-related acute gastroenteritis was between 35.2 and 59.4 million (applying the incidence rates obtained for small chlorinated systems and untreated private wells, respectively). Reynolds et al. (2008) reported that over 12 years in the United States, approximately 6.4 million annual waterborne illnesses were attributed to contaminated groundwater. In England and Wales, Smith et al. (2006) reported that between 1992 and 2003, outbreaks of waterborne, infectious intestinal disease was 35× greater among consumers served by private wells than those using public water supplies.

Data regarding viral concentrations in private well water is scarce. The percentage of viral positive samples during sampling campaigns varies widely depending on the sampling frequency, analytical methods, aquifer characteristics, and rainfall events. Sampling campaigns carried out by Borchardt et al. (2003) reported that 8 % (4/50) of 50 household wells in Wisconsin tested positive for viruses at least once per year when sampled four times a year. Enteric viruses were found by Borchardt et al. (2012) in 25 % of 1200 tap water samples collected from US municipalities supplied by untreated groundwater. Trimper (2010) analyzed 28 private wells in three Canadian provinces and found 58 % tested positive for viruses. Similarly, Allen et al. (2017) reported that 45 % (10/22) of drinking water–producing wells in fractured dolostone aquifers tested positive for human enteric viruses at least once in an eight-month period (six sampling events). The authors attributed this high frequency to shorter travel times to wells and larger capture zones in fractured rock aquifers.

Public health strategies for protecting domestic drinking water from wells generally assume that microbial transport will be sufficiently attenuated in the aquifer when there is sufficient distance between the wastewater disposal fields and drinking water wells. Most regulations therefore enforce horizontal setback distances between the point of infiltration and abstraction. Such distances should therefore be correlated with the residence time required to obtain good drinking water quality, i.e., a longer transport period in distance and time in accordance with regional geology. However, current policies are overwhelmingly lacking in such rationale. In Canada, the regulatory setback distance is set at 30 m (15 m in the province of Alberta), which is also the default value in the US (USEPA, 2022). Only a few specific provincial regulations introduce a rationale related to the direction of the hydraulic gradient and specific infiltration flow rates. In France, there is a single setback distance of 35 m (*Law on water and aquatic media n° 2006–1772, 2006 December 30th*). This distance is 50 m in Germany, and wells must be placed upgradient of septic systems (*Law on Water Resources*, *Wasserhaushaltsgesetz WHG*). Several modeling exercises have shown that regulatory setback distances are too low or too varied to be universally defined (Schijven et al., 2002; van der Wielen et al., 2006, 2008; Masciopinto et al., 2008; Trimper, 2010; Blaschke et al., 2016). Thus, the implementation of revised, non-arbitrary, and science-supported policies is imperative to ensure the protection of private water-production wells.

This absence of a scientific basis underlying existing regulatory setback distances stems essentially from a gap in scientific knowledge regarding the movement of viruses and pathogens through aquifers (Azadpour-Keeley and Ward, 2005; Gunnarsdottir et al., 2013). Numerous approaches have been proposed for modeling the fate of viruses in subsurface environments. The complex virus transport mechanisms are commonly represented in attachment–detachment models (Schijven and Hassanizadeh, 2000; Azadpour-Keeley and Ward, 2005; Torkzaban et al., 2006; Frohnert et al., 2014; Macías et al., 2017). Viral reduction in saturated porous media is governed by virus die-off, dilution, and retentive interactions with the solid substrate. The latter interactions are physically complex, encompassing mechanical processes, e.g., size exclusion, and electrostatic or hydrophobic solid surface–retention mechanisms (Jin and Flury, 2002). A key challenge is calibrating virus-reduction reactions and incorporating the hydrogeological variability of actual aquifers.

Although researchers have evaluated the influence of physicochemical properties of groundwater on inactivation rates and virus retention mechanisms, the quantitative assessment of the role of subsurface physical parameters, such as hydrogeological variability on virus persistence in groundwater, remains lacking. A few studies have illustrated the greater vulnerability of certain high-conductivity media to contamination, e.g., fractured rocks, karsts, and sand–gravel aquifers (Schijven and Hassanizadeh, 2000; Bhattacharjee et al., 2002; Hlavinek et al., 2008; Masciopinto et al., 2008; Macías et al., 2017). However, there is a lack of quantitative information related to identifying the predominant hydrogeological, environmental, and anthropogenic factors affecting subsurface viral reaction kinetics and the fate of concentration peaks in aquifers. This information is nonetheless critical for incorporating groundwater science into establishing setback distances. Improved setback distance policies require guidelines to address the critical question of the site-specific parameters that should be used to

define individual setback distances to protect against viral contamination. This study aims to model the relative importance of hydrodynamic and reaction parameters on the transport of viruses in aquifers and the associated health risks for private wells.

First, we use published field and laboratory-scale experimental data sets to develop and validate numerical solutions for modeling virus subsurface reactive transport using an analytical solution (diagnostic approach). In the second step, we apply a prognostic approach to the model to (1) analyze the penetration dynamics of virus concentration pulses in saturated porous media as a function of kinetic reaction coefficients; and (2) analyze the sensitivity of hydraulic parameters and kinetic reaction coefficients on the predicted viral risk. This study was designed to support risk-based policies where simulated virus transport is converted into health risk predictions by means of dose–response relationships. We compare risk predictions for a wide range of input parameters to the standard regulatory health risk target of 10^{-4} infections/person/year and a 30 m setback distance to highlight situations for which groundwater regulators must be attentive.

2. Methods

2.1. Conceptual model

We use a one-dimensional, laterally infinite, and fully saturated modeling domain. The hydraulic properties are homogeneous and isotropic, the flow is steady state, and we use a two-year predictive timeframe. We assume the mass transport problem is transient, and the input virus concentration is imposed at the source (Dirichlet-type boundary condition). Following Canadian regulations, which impose a 1.8 m depth between the infiltration trenches and the groundwater table, we position the strict boundary between the septic system and the aquifer (i.e., the viral source) at this depth for the conceptual mode. The viral concentrations at the source of the model must therefore account for virus removal in the disposal field, which has been reported as equal to 0–2 log (Hijnen et al., 2004; Dullemont et al., 2006; Eregno and Heistad, 2019). The septic tank itself removes a maximum of 0–2 log of viruses (Lusk et al., 2017; Adegoke and Stenstrom, 2019). Therefore, the total range for virus removal in septic systems is 0–4 log (see the review by Blaschke et al., 2016).

The viral source function is time variant and is calibrated using the amplitude and duration of a virus pulse emanating from the disposal field of a four-person residence during a single disease event. In the model, the duration of the disease event is fixed at 11 days, which is an average realistic value (Schijven et al., 1999). The viral concentration input into the septic system is calculated as the product of a sick human's fecal concentration and the daily individual fecal production (128 g/day) divided by the daily water consumption for the entire residence (1500 L/day). For rotaviruses, which are highly prevalent in Canada (Schuster et al., 2005), Anderson and Weber (2004) reported peak virus fecal concentrations up to 1010 to 1012/g during a disease event. This estimate provides a range of wastewater viral concentrations, before septic treatment, of 8.9–10.9 log/L. This estimate is conservative and assumes a constant concentration over the pulse duration. Usually, viral shedding decreases progressively after the peak. Bennett et al. (2020) report a one-log daily reduction over ten days. Thus, after 0–4 log removal in the septic system, viral concentrations added into the natural environment can vary between 4.9 and 10.9 log/L, or 7.9×10^4 and 7.9×10^9 viruses/L. This result agrees with the direct measurements by Charles et al. (2003) for rotavirus in treated domestic wastewater, i.e., 3–10.9 log/L. Previous modeling studies have made similar assumptions (Blaschke et al., 2016). The benchmark value retained for pulse concentrations at the source of the models is $C_0 = 9.2$ log/L $= 1.5 \times 10^9$ viruses/L, a conservative value without being in the maximum bracket of the calculated plausible range (7.9×10^{10} viruses/L). We assume that all viruses are infectious. We also investigate the sensitivity of our model to this input parameter.

2.2. Viral reaction model

The nature and the kinetics of the mechanisms responsible for pathogen removal in aquifers (chemical, electrostatic, and mechanical retentive interactions with solids) and their mathematical formulations have long been debated (e.g., for virus pathogens, Bitton and Marshall, 1980; Yates et al., 1985; Grant et al., 1993; Bales et al., 1995; Chrysikopoulos and Sim, 1996; Sim and Chrysikopoulos, 1996; Gerba and Smith, 2005; Jin and Flury, 2002; Azadpour-Keeley and Ward, 2005; Blanford et al., 2005; Tufenkji, 2007; Anders and Chrysikopoulos, 2009; Trimper, 2010; Bradbury et al., 2013). Pioneer virus adsorption experiments by Moore et al. (1981) suggested that polioviruses behave like solutes and can be modeled adequately by equilibrium sorption concepts. Later, these results were largely disproved by numerous continuous-flow sand-column experiments (Bales et al., 1993; Jin et al., 1997; Torkzaban et al., 2006; Frohnert et al., 2014; Betancourt et al., 2019) and some in situ experiments (Bales et al., 1995; Schijven et al., 1999; Blanford et al., 2005). Over the last two decades, a consensus has emerged that the interaction of viruses with a solid medium occurs at a lower rate than for solutes and cannot be approximated via an instantaneous equilibrium. These interactions are therefore represented using kinetic models. These models were first introduced in the 1960s and 1970s to reproduce the nonlinear interactions of organic compounds, e.g., pesticides, with the solid surfaces of organic matter and hydroxide minerals (Ogata and Banks, 1961; Lindstrom, 1976; Rao et al., 1979). Kinetic models also efficaciously predict the fate of pharmaceutical molecules in the natural environment (Nkedi-Kizza et al., 2006). Schijven et al. (1999) and Frohnert et al. (2014) demonstrated the ability of the kinetic model to reproduce viral responses obtained from in situ and laboratory experiments. Both studies concluded that optimal fits for measured temporal and spatial series of viral concentrations could be obtained using a *kinetic* rather than an *equilibrium* sorption model. We therefore use the fully kinetic sorption model as described by Schijven et al. (1999) and Frohnert et al. (2014).

In this model, the global interactions of viruses with solid surfaces are described by two interdependent first-order kinetic reactions, namely attachment and detachment (e.g., Schijven et al., 1999; Frohnert et al., 2014). The respective mass transfer rates for attachment and detachment are given by

$$r_a = -k_{att} C, \text{ and} \tag{1}$$

$$r_d = -k_{det} \frac{\rho_b}{\theta} S \tag{2}$$

where C [viruses L^{-3}] and S [viruses M^{-1}] are the concentrations of mobile and immobile viruses, respectively, k_{att} [T^{-1}] and k_{det} [T^{-1}] are respectively the attachment and detachment reaction coefficients, and θ [−] and ρ_b [$M.L^{-3}$] are porosity and dry medium density, respectively.

Additionally, in the porous media, viruses degrade because of the absence of both host organisms and viral metabolic activity (e.g., Jin and Flury, 2002). Although the mechanisms implied in this process remain poorly understood (Tufenkji, 2007), the inactivation of mobile viruses is well described by a first-order kinetic law [see review by Jin and Flury (2002)]. The description of immobile or attached virus inactivation kinetics requires field or sand-column experiments and is consequently less documented. However, authors have reported observations that the kinetics are related to a first-order problem (Hurst et al., 1980; Schijven et al., 1999; Frohnert et al., 2014; Macías et al., 2017). Reaction rates via the inactivation of mobile and immobile viruses are given respectively by

$$r_c = \frac{\partial C}{\partial t} = -\mu_l C, \text{ and} \tag{3}$$

$$r_s = \frac{\rho_b}{\theta} \frac{\partial S}{\partial t} = -\mu_s \frac{\rho_b}{\theta} S \tag{4}$$

where μ_l [T^{-1}] and μ_s [T^{-1}] are the inactivation coefficients of mobile and immobile viruses, respectively.

Finally, flow-induced and purely hydrodynamic mass transfer is governed by advection, which is the linear translation of water at a given pore velocity v [$L.T^{-1}$], and dispersion, a strongly scale-dependent empirical term (Schulze-Makuch, 2005), which accounts for the nonuniform pore-velocity fields.

The budget of virus mass transfers induced by the four reactions (Fig. 1) is thus given by the summation of eqs. 1–4. The total mass transfer rate of viruses in the saturated porous one-dimensional medium is obtained by integrating reaction-related and flow-induced mass transfer terms:

$$\frac{\partial C}{\partial t} = D\frac{\partial^2 C}{\partial x^2} - v\frac{\partial C}{\partial x} + r_a - r_d + r_c$$
$$= D\frac{\partial^2 C}{\partial x^2} - v\frac{\partial C}{\partial x} - K_{att}C + K_{det}\frac{\rho_b}{\theta}S - \mu_l C, \text{ and} \quad (5)$$

$$\frac{\rho_b}{\theta}\frac{\partial S}{\partial t} = -r_a + r_d + r_s = K_{att}C - K_{det}\frac{\rho_b}{\theta}S - \mu_s\frac{\rho_b}{\theta}S \quad (6)$$

where D [M^2T^{-1}] is the hydrodynamic dispersion coefficient.

As an alternative modeling approach, Blaschke et al. (2016) produced simplified first-order empirical analytical solutions calibrated using an extensive database of field measurements of virus concentrations (Pang, 2009). Advantageous for practical purposes, this approach accurately approximates the kinetics of virus removal. However, its validity scope may be restricted to the specific parameters, scale, and time regime of the calibration database and conceptual model, as it fails to reproduce the concentration data obtained from transient in situ and lab experiments, which are not first-order behaviors.

The reactive non-conservative flow problem was solved numerically through a finite-element method in a single dimension using the FEFLOW code (Diersch, 2014).

2.3. Health risk calculations

The health risk at the well was calculated using a dose–response relationship for rotavirus (Eq. 8), an approach used by Health Canada to develop guidelines for virus removal from drinking water (Health Canada, 2019). The daily concentration (C) of viruses in a domestic well was obtained from our model calculations. Assuming a water consumption of 1.5 L/day per person, we can calculate a daily viral dose (D, number of viruses ingested; Eq. 7) and a daily probability of infection (P_k; Eq. 8).

$$D = 1.5\ C, \text{ and} \quad (7)$$

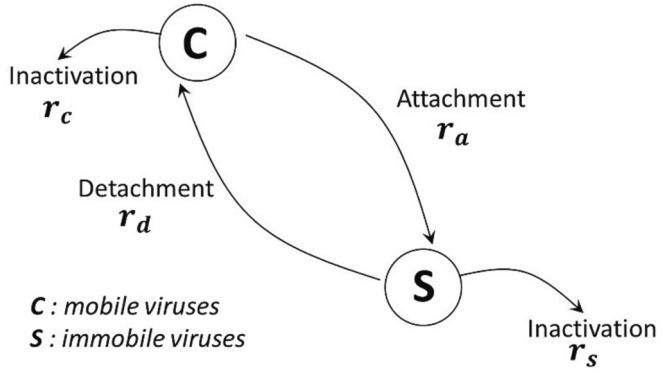


Fig. 1. Conceptual model of reactions producing mass transfers of viruses. The four reactions are time dependent. Note: r_x is the mass transfer rate by reaction x; see eqs. 1–4.

$$P_k = 1 - \left[1 + \frac{D}{\beta}\right]^{-\alpha} \quad (8)$$

where $\alpha = 0.265$ and $\beta = 0.4415$ are the empirical parameters of infectiousness for rotavirus. We assume that there is no secondary spread of infection. We selected rotavirus for our health risk assessment (1) to be consistent with Canadian regulations; (2) because of its regular occurrence in Canadian private wells (Schuster et al., 2005; Trimper, 2010); and (3) to align with the chosen model parameters. Indeed, the input viral concentrations are based on rotavirus and the kinetic parameter values published for experiments using MS2 coliphages and PRD1 bacteriophages, both rotavirus surrogates (Azadpour-Keeley et al., 2003).

Finally, the annual risk (P_{year}) is calculated from the product of daily risks (Eq. 9):

$$P_{year} = 1 - \prod_{k=1}^{365}(1 - P_k) \quad (9)$$

3. Model validation

3.1. Virus breakthrough curves

Measured breakthrough curves (BTCs, concentration time series at various distances) are typically used to obtain inverse estimates of transport parameters (e.g., Ratha et al., 2009). Note that the dispersivity of suspended particles like viruses is a size dependent parameter as exposed by Chrysikopoulos and Katzourakis (2015). In this study, we used BTC to validate the transport model and evaluate the influence of distinct transport parameters and reaction mechanisms (Fig. 2). Fig. 2 portrays BTCs associated with various reactive transport models published by Schijven et al. (1999) on the basis of the series of analytical solutions submitted by Toride et al. (1995). The observed long tail is highly characteristic of kinetic transport models (Fig. 2E, F, H), in which a very slow virus attenuation rate is the consequence of prolonged virus detachment from the solid phase. Therefore, the differences between the equilibrium and kinetic reactive models are particularly pronounced in long time series. Another diagnostic feature is the change in slope between the long tail and the peak, with a transition marked by a vertical offset ("shoulder") reflecting a short intermediate stage during which the reduction rate is very high; this shoulder likely reflects the prominence of attachment as a reducing mechanism.

A primary qualitative step for validating our numerical model involves verifying whether it can reproduce the characteristic features of BTCs published by Schijven et al. (1999) for a kinetic reactive behavior (Fig. 2E, F, H). Breakthrough curves obtained via the numerical model are shown in Fig. 3. The key elements to note are that (1) the long-term behavior (long tail) is highly controlled by the immobile inactivation coefficient μ_s, as previously mentioned by Schijven et al. (1999); (2) that in contrast, the attachment coefficient K_{att} controls the initial response involving the peak reduction amplitude and the overall shape of the curve, corroborating the Schijven observations in Fig. 2H; (3) the transition between peak and tail, i.e., the offset ("shoulder") amplitude, is linearly proportional to the detachment coefficient K_{det}, as is the vertical offset of the tail. Note that the slope of the tail in Fig. 2E and F is not affected by K_{det}, which disproves the statement of Schijven et al. (1999).

This exploration analysis of kinetic transport responses exposes the complex dynamics of viral reduction where the four reactions are interdependent while successively exerting a dominant influence on the overall viral reduction. As a general rule, attachment determines the early reduction kinetics, whereas long-term persistence is ruled essentially by mobile virus inactivation, detachment, and markedly by immobile virus inactivation.

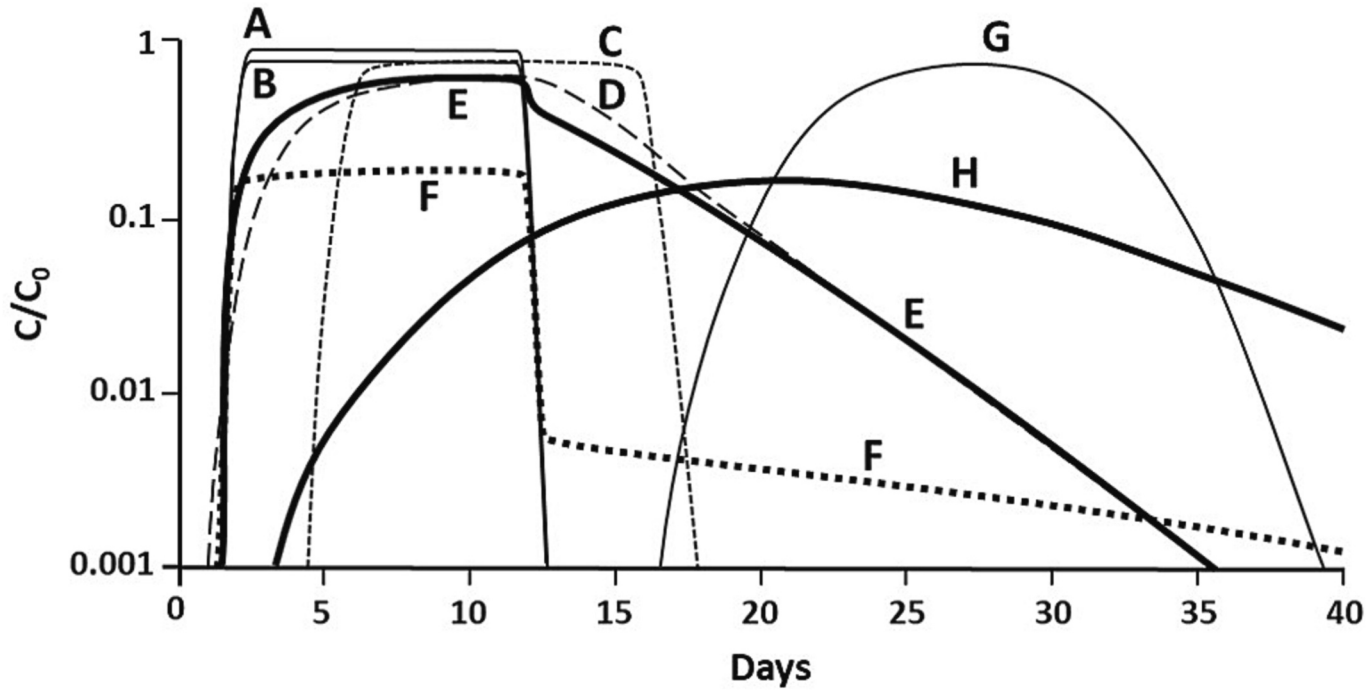


Fig. 2. Theoretical breakthrough curves predicted for transport models involving various mass transfer mechanisms: A) tracer (nonreactive, purely advective – dispersive transport); B) same model but with first-order degradation; C) equilibrium sorption reactive transport (valid for solutes); D) and G), model C with a high dispersion or a high retarding factor, respectively; E), F), and H), two-site kinetic reactive transport models, valid for organic compounds (e.g., pesticides and pharmaceutical products), with low detachment, high detachment, and high attachment, respectively. Pulses are injected over ten days, 3 m upstream, at 1.5 m/d pore velocity. Modified from Schijven et al. (1999).

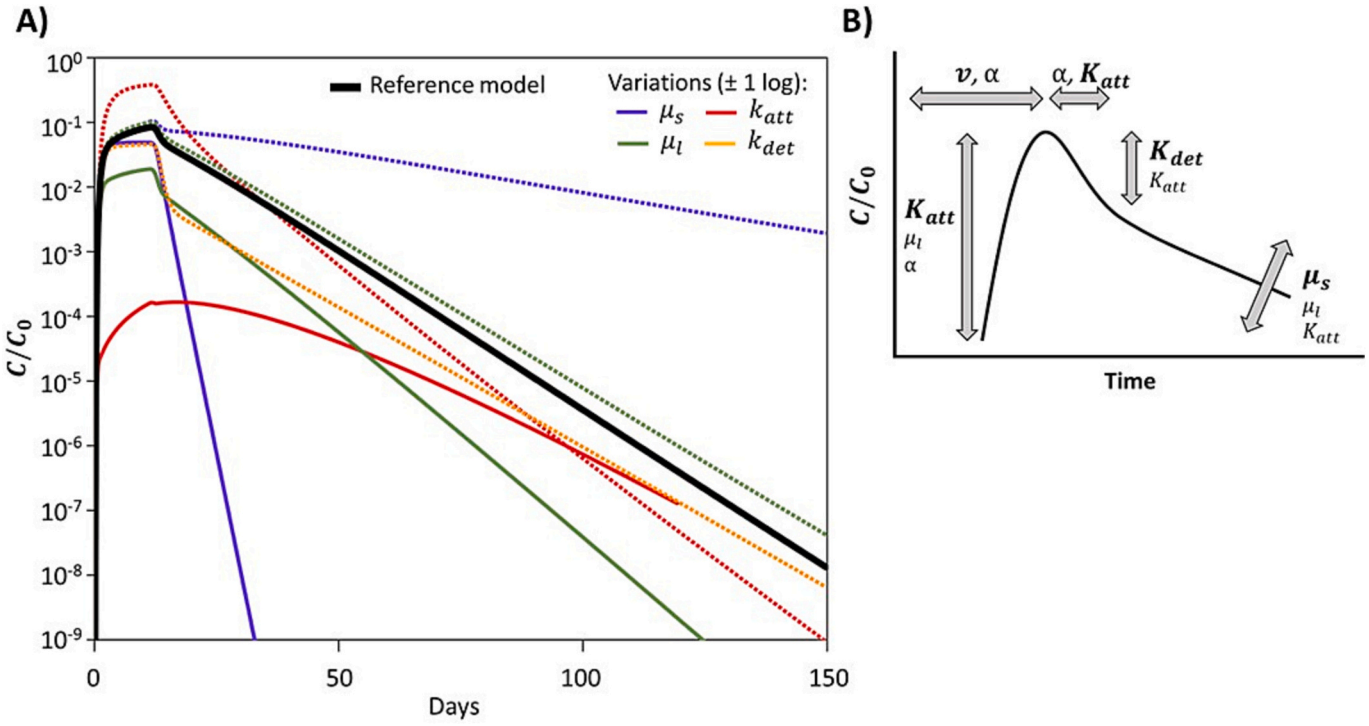


Fig. 3. Influence of reaction coefficients K_{att}, K_{det}, μ_l, and μ_s on virus breakthrough curves (C/C_0) for the fully kinetic model. A) Numerical simulations (3 m downstream of the injection point, 11-day injection pulse). The amplitude of variations of the parameters is one-log greater (dotted lines) and less (solid lines) than the reference model (except for K_{det} for which only the lower limit is presented because of mathematical limits). The reference model values are $K_{att} = \mathbf{1}/\mathbf{d}, K_{det} = \mathbf{0.1}/\mathrm{d}, \mu_l = \mathbf{0.1}/\mathrm{d}$, **and** $\mu_s = \mathbf{0.1}/\mathrm{d}$; the flow parameters are $v = \mathbf{0.1}$ m/d, $\alpha = \mathbf{2}$ m, **and** $\theta = \mathbf{0.3}$.). B) Schematic of the theoretical influence of the reaction coefficients on virus breakthrough curves.

3.2. Analytical validation

Our kinetic reactive transport model, also referred to as the *mobile–immobile fully kinetic model,* does not have a published analytical solution; however, Toride et al. (1995) offer a generic form, referred to as the *two-site equilibrium/kinetic sorption model*. The solution assumes 1) equal attachment and detachment coefficients; and 2) the inactivation coefficients for the mobile and immobile virus phases are equal. This one-dimensional analytical model considers a distribution function between kinetic (attachment–detachment) and equilibrium (Henry isotherm) sorption sites. Although this sorption model was designed for pesticide transport, we use it for validation because its implementation in FEFLOW is very similar to the *full kinetic model* used for viruses. The simulation was carried out for a 300-day pulse source. Results are given in Fig. 4 for breakthrough curves at a distance of 10 m from the source and for various inactivation rates—expressed in terms of the dimensionless parameter $\Psi = \mu \cdot L/v$, where L and v are the distance and pore velocity, respectively. Interestingly, the numerical code reproduces the theoretical response appropriately, as predicted by the analytical solution of Toride et al. (1995) for both short- and long-term transport.

3.3. Field experimental validation

To our knowledge, only three studies have reported on experimental data sets of virus transport under actual aquifer conditions: Bales et al. (1995), Schijven et al. (1999), and Blanford et al. (2005). We selected the data set of Schijven et al. (1999) to validate our model, as their study was carried out in fully saturated media, and the data sets are of high quality. Schijven et al. (1999) analyzed the short- to long-term propagation of MS2 and PRD1 pulses injected into a sandy aquifer by monitoring breakthrough curves in six wells. Their test duration was 120 days, and the monitoring wells were spatially distributed along the linear flow path starting from the injection well and constrained by a far-field high-rate pumping well (63 m, 330 m^3/h). Sampling in monitoring wells relied on a low-flow pumping method (4 L/min). The granular aquifer was composed of a 10 m thick, high-hydraulic conductivity (est. 12 m/d), grossly homogeneous and isotropic, eolian dune sand layer, which overlays a low hydraulic conductivity (4 m/day) fine grain sand layer (unpumped). The pulse injection involved maintaining a constant virus concentration within a 10 × 15 m recharge compartment over 11 days (see Schijven et al., 1999 for details). Note that the virus injection from the surface over a 150 m^2 area is spatially diffuse rather than a punctual source at the scale of the experiment. This diffuse sourcing may smooth the shape of the peaks measured in vertical monitoring wells. Schijven et al. (1999) estimated flow and transport parameters through an inverse approach using tracer breakthrough curves. To estimate the viral transport parameters, Schijven et al. used a fully kinetic reactive model identical to ours. The mobile viral inactivation coefficient μ_l was measured from direct batch experiments, K_{att} and μ_s were derived from inverse calibrations of some chosen segments of breakthrough curves with ad hoc analytical solutions making linear postulates. Finally, K_{det} was estimated by inverse calibration using an unpublished analytical solution modified from the abovementioned generic solution given by Toride et al. (1995).

Here, we calibrate the numerical model using input parameter values equal to those of Schijven et al. (1999), except for the attachment rate (set here at 1.5 per day rather than 4 per day). We obtained results for MS2 at four wells (Fig. 5). The observed long tails are highly characteristic of kinetic transport models, as explained above, and the numerical model correctly reproduces this tail. Such predictions of persistent low virus concentrations after long residence times fit very well with the observations in the three wells closer to the source. We lack long-term data for the fourth well (10 m); however, we can observe a departure from the theoretical curve before 50 days, which may be

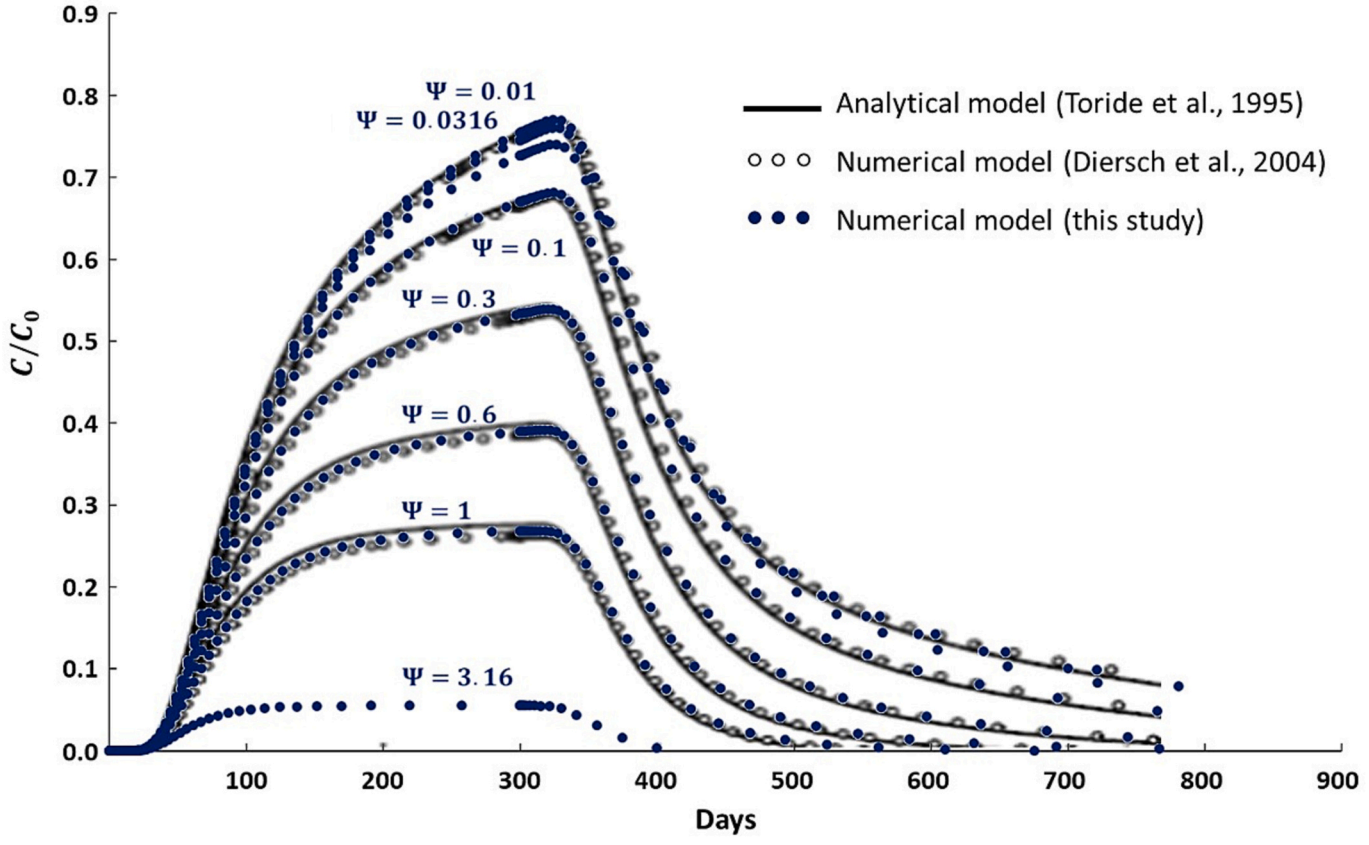


Fig. 4. Comparison of simulated breakthrough curves obtained using numerical and analytical solutions for the two-site equilibrium/kinetic sorption model. $\Psi = \mu . L/v$ is a dimensionless parameter. Modified from Diersch (2014).

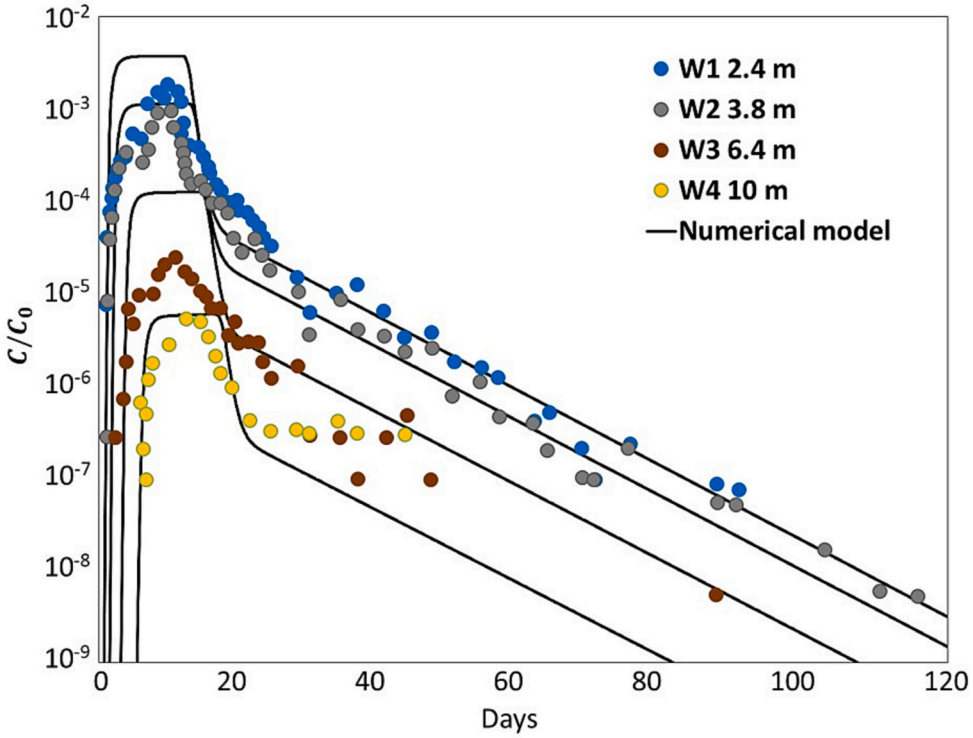


Fig. 5. Comparison of modeled and measured MS2 breakthrough curves of field test experiment (Schijven et al., 1999). The simulation parameters are $v_D = 0.5$ m/d, $\alpha = 0.01$ m, $\theta = 0.35$, $K_{att} = 1.26$/d, $K_{det} = 0.0008$/d, $\mu_l = 0.03$/d, and $\mu_s = 0.09$/d.

attributed to spatially inconsistent reactive parameters (kinetic coefficients). This may reflect either changes in the physical properties of the solid medium or changes in the physicochemical properties of the groundwater (Jin and Flury, 2002). The poorer fit in the short-term (*syn*-peak segment) observed in Fig. 5 relates to divergent configurations of the source sensu stricto rather than to transport. As mentioned above, the experimental process involves viral infiltration into the aquifer over a large surface area, which likely induces deformations of the peak's shape. Moreover, viral concentrations vary by half an order of magnitude because of experimental variability (Schijven et al., 1999). In contrast, for our validation work, the numerical model includes a Neuman-type source, i.e., fixed mass flux, for optimizing model fit, in the form of a discrete Boolean function with three levels: zero mass flux ($t < 0$), constant mass flux ($0 < t < 11$ d), and zero mass flux ($t > 11$ d).

3.4. Laboratory experimental validation

We also applied the laboratory experiments of Torkzaban et al. (2006) to provide additional model validation. The experimental setting is a continuous-flow, 23-cm-long column of saturated sand. Torkzaban et al. (2006) performed an inverse calibration of attachment and detachment coefficients using a numerical 1D *mobile–immobile fully kinetic* type model analogous to ours. We used the exact values provided in Torkzaban et al. (2006) to validate our model. The results, displayed in Fig. 6, show that the numerical model reproduces the experimental data perfectly.

4. Results

4.1. Selection of kinetic reaction coefficients

The reaction coefficients for the attachment, detachment, and inactivation of the mobile and immobile viruses are calibrated using values estimated from the scientific literature (Fig. 7). The kinetic coefficients for the attachment, detachment, and immobile virus inactivation are

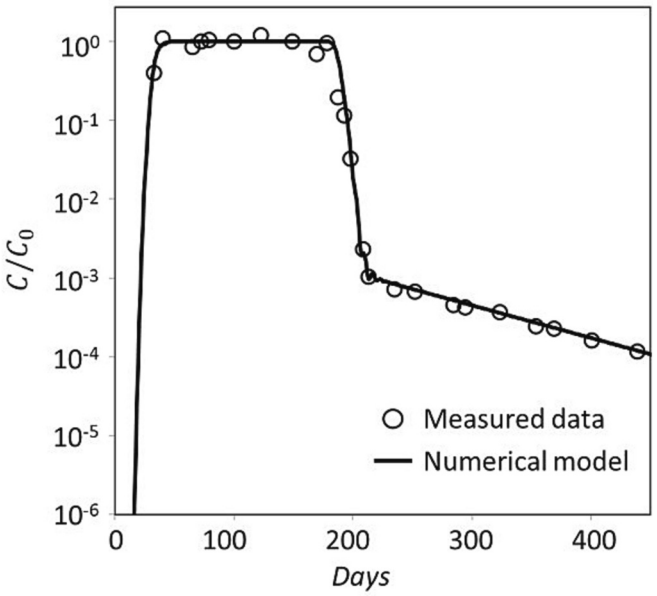


Fig. 6. Comparison of the modeled and measured MS2 breakthrough curves of the laboratory sand-column experiment (Torkzaban et al., 2006). The simulation parameters are $v_D = \mathbf{4.01}$ m/d, $\alpha = \mathbf{0.002}$ m, $\theta = \mathbf{0.41}$, $K_{att} = \mathbf{0.072}$/d, $K_{det} = \mathbf{13.68}$ /d, and $\mu_l = \mu_s = \mathbf{0.042}$ /d.

obtained by the inversion of temporal and spatial series of concentrations measured in saturated sand-column laboratory experiments, except for an in situ study by Schijven et al. (1999), which used kinetic reactive transport analytical and numerical models. In contrast, the inactivation kinetic of mobile virus is measured directly using batch tests (no flow) or chamber studies (continuous flow; Azadpour-Keeley and Ward, 2005), which explains the higher number of references.

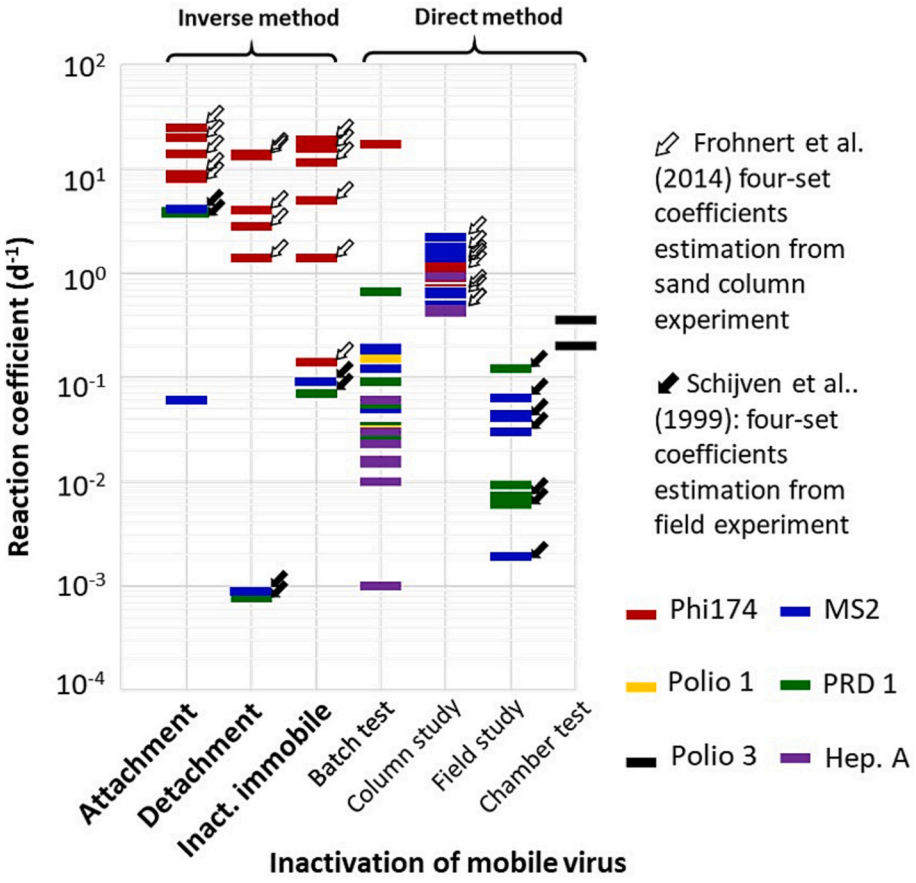


Fig. 7. Compilation of published reactions kinetic coefficients estimated from experiments. The inverse method is a curve-fitting using kinetic reactive models. (Additional references: O'Brien and Newman, 1977; Hurst et al., 1980; Keswick et al., 1982; Yates et al., 1985; Powelson et al., 1991; Nasser et al., 1993; Sobsey et al., 1995; Blanc and Nasser, 1996; Jin et al., 1997; Nasser and Oman, 1999).

Methodological biases and differences among the tested viruses produce a highly variable output. Methodological bias initially occurs through the differing conditions of the batch experiments: water temperature, pH, ionic strength, and the presence or absence of sandy or loamy material in the batch reactors (unspecified in Fig. 7). In the latter case, it is suspected that inactivation coefficients are overestimated, as the measured kinetic rate is not only the inactivation rate but rather corresponds to the total effective reduction rate, which includes attachment, detachment, and immobile virus inactivation. Marked discrepancies are also observed between the only two studies that estimated the four kinetic coefficients (K_{att}, K_{det}, μ_l, and μ_s) by inversion of field test data (Schijven et al., 1999) and column test data (Frohnert et al., 2014). In similar inversion models, the kinetic coefficients estimated through field tests are systematically lower than those estimated via a column test, with major differences between inactivation coefficients (2–3 log) and a marked difference between detachment coefficient values (up to 4 log, see Fig. 7). Estimates from Schijven's field test give K_{att}/K_{det} ratios up to 4500 for the MS2 and PRD1 viruses, which are disproportionately higher than the ratios (0.5 and 20, respectively) obtained by Frohnert et al. (2014) using a lab column test with PhiX174. These discrepancies may be attributed to 1) real aquifer pore conditions versus the ideal homogeneous sand column; 2) methodological imprecision (curve-fitting process); or, at least partly, 3) natural variability (virus types, groundwater properties). Regardless, kinetic coefficient estimates from the field tests of Schijven et al. (1999) are considered more realistic and are used hereafter as benchmarks for calibrating the model.

This compilation highlights the serious methodological challenges explaining the lack of quantitative constraints on determining viral reduction under actual subsurface transport conditions, particularly the implied kinetics of the distinct reactions. Despite the major discrepancies among the published values, we do note the following trends: 1) the inactivation of immobile viruses is greater or sensibly equal to the inactivation of mobile viruses; and 2) the variability of the immobile/mobile inactivation coefficients ratio is low (within an order of magnitude).

4.2. *Penetration and persistence of viral pulses in saturated porous media*

We investigated the dynamics of attenuation and propagation of viral pulses in saturated porous media using a systematic analysis (Monte Carlo process, 1200 runs) of the interdependent influences of the four input kinetic parameters, namely attachment, detachment, and mobile and immobile virus inactivation coefficients, respectively, K_{att}, K_{det}, μ_l, and μ_s. This analysis highlights an extreme variability of virus behavior as a consequence of the high variability of the values of these coefficients reported from experimental works (Fig. 7). For example, for values of hydrodynamic parameters typical of a sandy aquifer (Darcy velocity equal to 0.1 m/d and 30 % porosity), the reduction of the viral peak after 300 days varies from 1 to 15 log at a penetration between 1 and 60 m. The penetration of virus pulses is influenced in the first instance by the K_{att}/K_{det} ratio, whereas it is less affected by μ_l and μ_s. For the same configuration of hydrodynamic parameters as above, low K_{att}/K_{det} (below 10) models predict peak penetration between 10 and 60 m, whereas it remains below 5 m for ratios higher than 100. In contrast, μ_s exerts a marked positive influence on reducing viral peaks (Fig. 8). For values of μ_s as low as 0.001 /d, peak attenuation after 300 days is very low (<4 log), regardless of the value of μ_l.

It is worth noting that, beyond these overall trends, the dynamics of viral subsurface reactive transport are nonlinear, and the reactions are strongly interdependent. For instance, the effect of immobile virus inactivation on peak reduction increases with the K_{att}/K_{det} ratio. This pattern occurs because a significant accumulation of immobile viruses is retained within the solid medium during the passage of the pulse owing to a high K_{att}. This retention implies a minimal release of viruses into the fluid by detachment because of a low K_{det}, such that immobile virus concentrations are maintained and their inactivation determines the long-term release potential into the fluid. In cases where the K_{att}/K_{det} ratio is high and μ_s is low—a realistic configuration according to field experiments by Schijven et al. (1999)—the lack of significant inactivation of the attached immobile viral load generates the protracted release of viruses into the fluid, thus leading to their persistence in the aquifer, although at low concentrations. Such a low residual virus concentration in groundwater has been observed previously in experimental breakthrough curves (Blanford et al., 1995); we submit that it is the direct consequence of protracted viral detachment with low immobile inactivation kinetics. Although these residual concentrations are strongly reduced, the impact on health risk can remain non-negligible, as explained below.

The release of a viral load into a fluid by detachment occurs predominantly directly upstream of the peak—where large concentrations of immobile virus may have been attached during the passage of the pulse. This release by detachment is prone to producing a retarding effect on the pulse propagation and markedly restrains its penetration into the aquifer. In extreme cases where high attachment combines with limited immobile inactivation, this phenomenon may generate an apparent retrograde transport during the weeks following the viral pulse infiltrating from wastewater disposal fields, as in Figs. 8 (dotted line) and 9. The decomposition analysis of mass transfer budgets (see Fig. 10) provides visual evidence that such a delaying effect is caused by specific conditions upstream of the peak (blue arrow in Fig. 10), where the reaction budget increases and even becomes positive (dark blue curve in Fig. 10) because of the predominance of positive mass transfers by detachment over negative mass transfer by attachment combined with mobile inactivation. An apparent reverse transport effect occurs when this positive balance (dark blue curve) is even greater than the negative mass transfer by transport (dark green curve), such that storage is positive (Fig. 10).

This systematic analysis of virus transport dynamics controlled by reaction kinetics highlights that 1) the detachment-induced release of viruses into the fluid, upstream of the peak, induces a delay that may be marked or protracted depending on the kinetic parameters of the immobile phase, namely, the immobile inactivation and detachment; 2) the long-term persistence of viruses in groundwater is essentially determined by these two kinetic parameters of the immobile phase, which corroborates the slope of the viral BTC tail being proportional to μ_s, as explained above). The consequence is the generation of residual viruses having potential health risks, as discussed further below; and 3) most importantly, in light of such high sensitivity of subsurface viral peak penetration and persistence of kinetic parameters, the insufficient amount of quantitative knowledge demonstrated above prevents a robust prediction of the fate of viruses in aquifers. An improved determination of viral kinetic parameters from field experiments is thus an essential research priority.

4.3. Health risk sensitivity to kinetic reaction coefficients

The sensitivity approach quantifies the influence of changes in the model's input parameters on target output parameters (see the detailed description in Doherty, 2015, 2018). Such a methodology typically aims to compare the relative sensitivities of selected input parameters and, in doing so, decipher those parameters controlling the phenomenon of interest. Annual health risk predictions— the output parameter—are modeled for various values of kinetic reaction coefficients—the input parameters—within the ranges of the experimental values compiled in Fig. 7. Fig. 11 presents the resulting values relative to the standard regulatory benchmarks of 10^{-4} risk (1 infection/10^4 persons/year) and a 30 m setback distance, the default regulation in most western countries. A *danger zone* is present where the health risk exceeds the 10^{-4} regulatory target. We define six scenarios (Table 1) to cover the real-world behavior variability (viral resistance and kinetic parameters). In model 1, the low K_{att}/K_{det} ratio associated with low inactivation coefficients produces a maximum pulse penetration into the aquifer and minimal reduction, leading to maximum risk. Other models represent

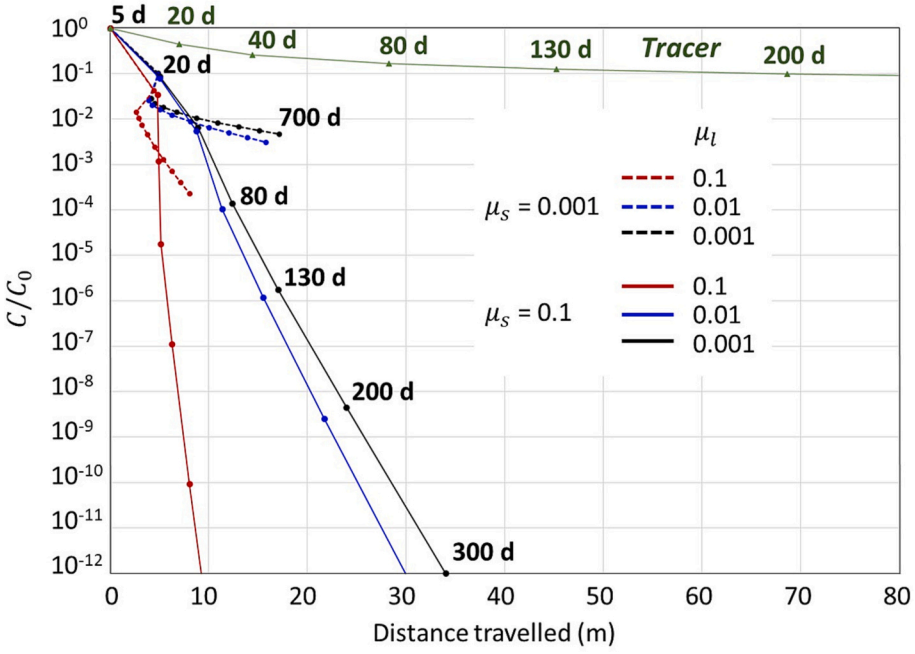


Fig. 8. Influence of the immobile virus inactivation coefficient on the reduction of viral peaks and viral penetration within the porous medium. The tracer is a nonreactive, purely advective–dispersive transport. The simulation parameters are $v_D = 0.1$ m/d, $\alpha = 2$ m, $\theta = 0.3$, $K_{att} = 0.1$ /d, and $K_{det} = 0.01$ /d.

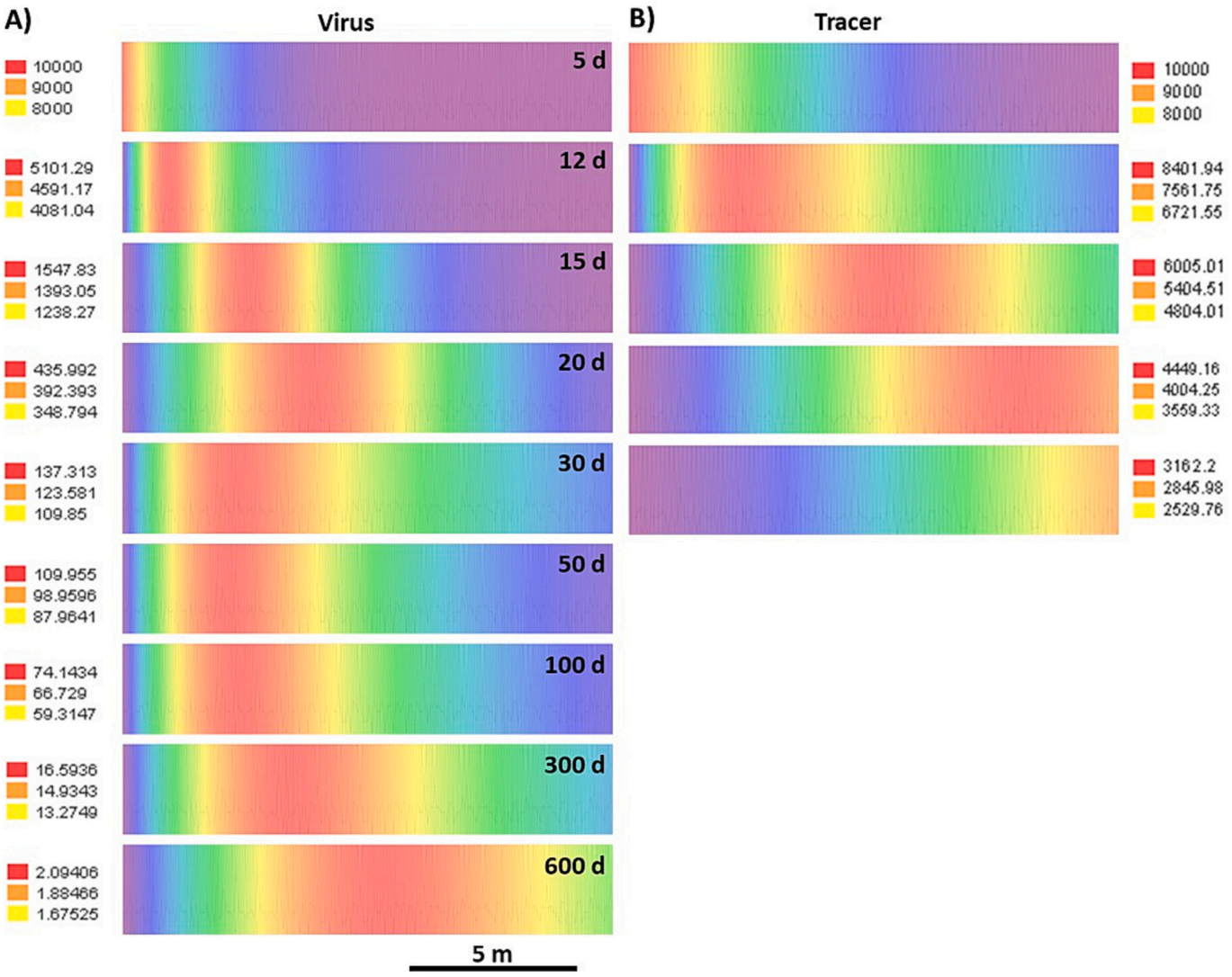


Fig. 9. Simulation pulse propagation for A) virus and B) tracer. The color chart is an equal range type (recalculated at each step for visual quality purposes; uncharted green to blue colors correspond to low to null concentrations, respectively. Note the apparent retrograde movement of viruses (20–30 days) reflecting the release (detachment) of previously attached viruses on the back of the peak. Pulses are injected at the left-hand boundary. The tracer is a nonreactive, purely advective–dispersive transport. The simulation parameters are $v_D = 0.1$ m/d, $\alpha = 2$ m, $\theta = 0.3$, $K_{att} = 0.1$ /d, $K_{det} = 0.01$ /d, $\mu_l = 0.1$/d, and $\mu_s = 0.001$/d.

intermediate to low virus persistence and penetration, including the experimental values from Schijven et al. (1999).

Within the real-world ranges of viral kinetic coefficients (and realistic flow parameters), the annual risk variability is marked and may likely exceed health standards. Models parameterized for maximum virus persistence (models 1 and 6) predict that attaining the 10^{-4} risk threshold requires a regulatory distance >30 m: respectively, 47 m and >> 100 m (not presented in Fig. 11). In the extreme case of model 1, the predicted risk remains 100 % at 100 m. This model illustrates conditions where the attachment–detachment dynamics are ineffective in immobilizing the viruses on the solid medium, which results in the deep penetration of the viral pulse into the aquifer (85 m after 1 year versus 121 m for a nonreactive tracer), combined with very slow virus die-off kinetics (2 log reduction of the peak after 1 year). As explained above, such conditions have not been observed, although they are possible. Models 2 and 3, parameterized respectively using the MS2 and PRD1 properties estimated by Schijven's field test, predict 100 % risk below 10 m and a rapid decrease, reaching the 10^{-4} target after 15 m. Note that the Darcy velocity used for this sensitivity analysis is significantly less than that of the Schijven et al. experiment (0.1 versus 1.57 m/d), such that the experiment's actual risk estimate is expectedly much higher (see the section below discussing the Darcy velocity sensitivity analysis).

The sensitivity of annual health risk models to viral attachment and detachment input values is illustrated in Fig. 12 for a 30 m benchmark setback distance. This analysis illustrates that the risk is essentially determined by attachment rather than detachment, within the range of experimental values compiled in Fig. 7. As expected, attachment is positively related to risk, whereas detachment shows a negative relationship to risk. Moreover, below $K_{att} = 1$ /d, the risk at 30 m is greater than the 10^{-4} threshold regardless of the detachment coefficient. In contrast, risk is always low for K_{att} values of 8/d or more. Between these two values, the detachment coefficient exerts a non-negligible influence on risk, albeit it is less sensitive than the attachment coefficient. This interpretative framework is nonuniversal and depends on the values set for mobile and immobile virus inactivation coefficients—in this case, both are identical at 0.01 /d—although these parameters exhibit low variability (Fig. 7) and are likely not a significant source of imprecision. Fig. 12 reveals the difficulty of rigorously quantifying the individual sensitivity of reaction coefficients because of their interdependence. Indeed, the sensitivity value for attachment, as given by the log ratio of change in K_{att} to the change in induced risk, increases with K_{det}. The K_{att} sensitivity, defined as the log-scale change in the risk value (output)

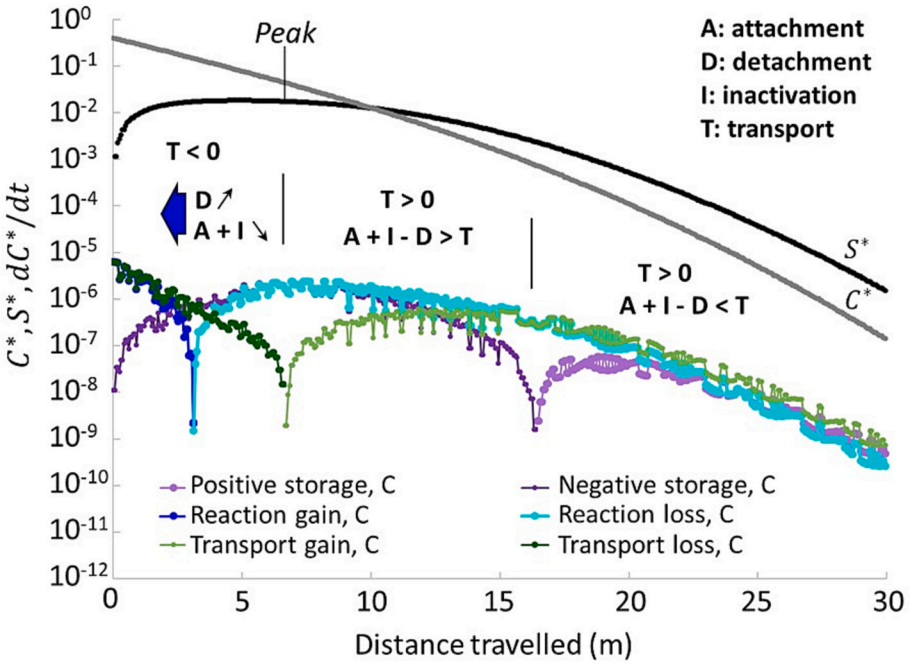


Fig. 10. Mass transfer budget decomposition along the longitudinal profile after 25 days (same model as shown in Fig. 9). Transport mass changes (T) are by advection and dispersion. Only the inactivation of mobile viruses (I) is considered. The storage gain or loss corresponds to the balance of transport and reactions (T – [A + I – D]). C^* (gray line) and S^* (black line) are respectively mobile and immobile virus concentrations normalized to the source concentration (C_0). Mass transfers are in d^{-1}.

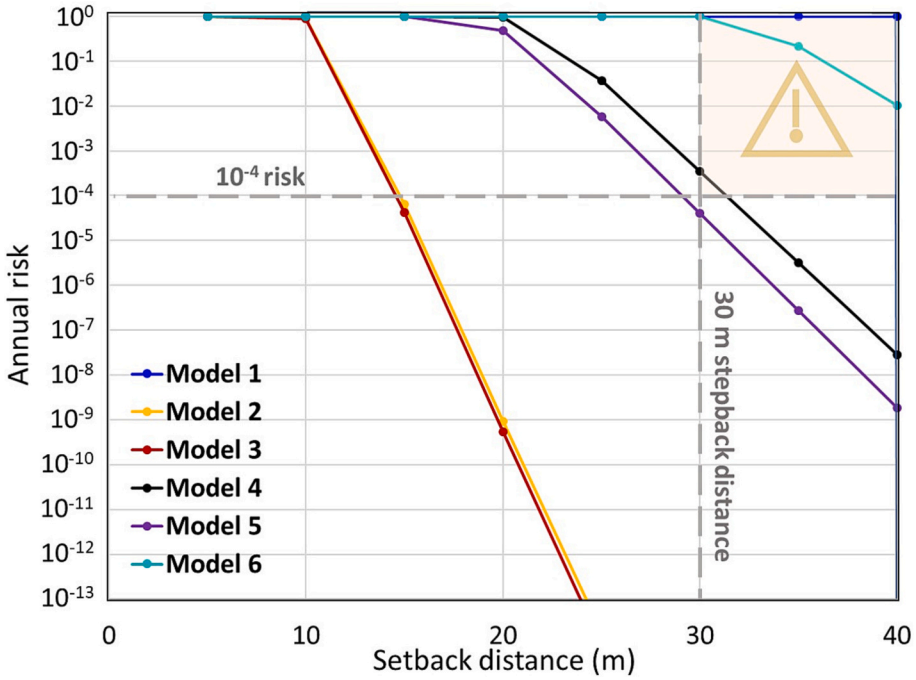


Fig. 11. Simulation results for annual health risk predictions as a function of setback distances for selected values of kinetic reaction coefficients (see Table 1). The simulation parameters are $v_D = 0.1$ m/j, $\alpha = 2$ m, and $\theta = 0.3$. The shaded zone with a warning symbol corresponds to a health risk exceeding the 10^{-4} threshold of the regulatory setback distances, i.e., the danger zone.

induced by a one-log change in K_{att} (input), is equal to 16 at $K_{det} = 10^{-3}$/d and 23 at $K_{det} = 10^{-1}$/d. In turn, the K_{det} sensitivity is between 10 and 11 for K_{att} within 0.1 to 10/d.

4.4. Health risk sensitivity to the hydraulic gradient and hydraulic conductivity

The effects of the flow parameters of hydraulic gradient i [−] and conductivity K [$L{\cdot}T^{-1}$] are expressed interchangeably in terms of the Darcy velocity v_D, following Darcy's law $v_D = -K{\cdot}i$. These parameters determine the advection term of transport. Darcy velocity is the groundwater volumetric flow through a unit transmissive surface; it is proportional to the pore velocity v as $v_D = v{\cdot}\theta$, where θ is the porosity. The hydraulic gradient used in the models varies between 0.001 (plains) and 0.1 (mountains), and the hydraulic conductivity values used in the models range between 10^{-6} and 10^{-3} m/s (0.0864–86.4 m/d), which grossly encompasses surficial hard rock aquifers and sandy, granular aquifers. In the case of hard rock aquifers, a distinction should be made between the rock mass conductivity of minor fracture networks, which behave similarly to a continuous porous medium (Ferroud et al., 2019),

Table 1
Kinetic reactions coefficient used in the models.

Model name	Characteristics	Virus persistance in GW	Coefficient values, /d			
			K_{att}	K_{det}	μ_l	μ_s
Model 1	Minimum reduction, maximum propagation - Maximum risk	Very high	0.1	0.1	0.001	0.01
Model 2	MS2 coefficients obtained in-situ by Schijven et al. (1999)	Low	4	0.0009	0.03	0.09
Model 3	PRD1 coefficients obtained in-situ by Schijven et al. (1999)	Low	4	0.0007	0.12	0.07
Model 4	Intermediate values	Medium	1	0.01	0.03	0.09
Model 5	Intermediate values	Medium	1	0.001	0.03	0.09
Model 6	Intermediate values	Medium	1	0.1	0.03	0.09

Other non-hydrodynamic parameters of the models: contamination is 11 days-long, virus source concentration is 9.2 log/L, Beta-Poisson model, water consumption is 1.5 L/d.

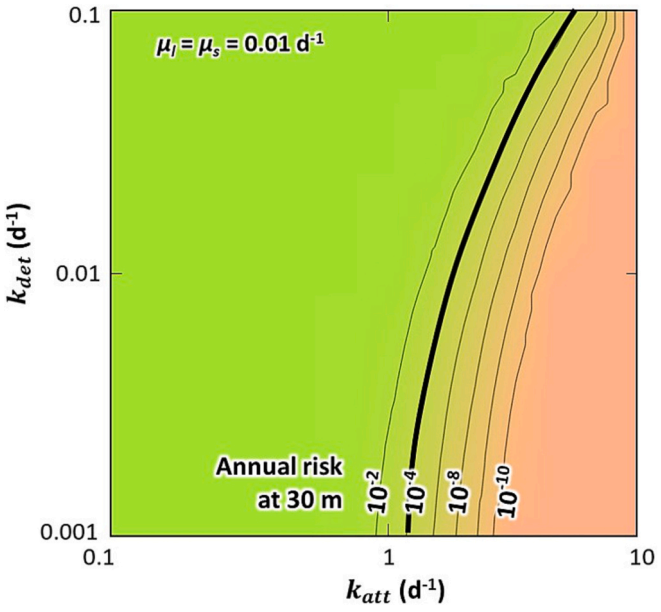


Fig. 12. Sensitivity of annual health risk at a 30 m setback distance to attachment and detachment coefficient input parameters. The simulation parameters are $v_D = 0.1$ m/d, $\alpha = 2$ m, and $\theta = 0.3$.

and the conductivity of discrete fault drains, which may be extremely high (e.g., Worthington et al., 2016). The upper range of 10^{-3} m/s retained in this study aims to include the conductivity in discrete drains. Thus in our models, we use values of v_D that range from 8.64×10^{-5} to 8.64 m/d to encompass the natural variability of the hydraulic gradient and conductivity parameters. The temporal and spatial time series of virus concentrations obtained from simulations are converted into annual health risk values through the above-described methodology.

Fig. 13A presents the risk–distance diagram for various Darcy velocities between 8.64×10^{-3} and 0.864 m/d for two distinct sets of viral reaction coefficients. These data are for models 2 and 4 (Table 1), the MS2 values of Schijven et al.'s field experiment, and an intermediate virus resistance configuration, respectively. This analysis demonstrates an extreme sensitivity of the annual health risk to v_D, i.e., to hydraulic gradient and conductivity. Therefore for the highest v_D(the viral pulse propagates rapidly via advection), the health risk decreases the slowest with distance from the viral source (the lowest slopes of curves in Fig. 13A). This pattern likely reflects the positive influence of velocity on pulse dispersion. The predictive risk simulations using a benchmark 30 m setback distance are displayed in Fig. 13B for selected viral reaction coefficients: models 2, 4, and 6 (Table 1). The risk sensitivity to v_D is illustrated as the stabilized slope of the curves (lower linear part). This figure demonstrates that this sensitivity is markedly high, around 25 log, and is obviously invariant in regard to the viral reactive properties. Thus, a 1-log increase in v_D induces a massive 25-log increase in risk. Regardless of virus type and removal properties, the health risk is predominantly controlled by the hydrodynamic transport parameters of hydraulic gradient and conductivity. Fig. 13B illustrates that for Darcy velocities >1, i.e., any pore velocities >3.3 m/d, assuming a porosity of 0.3 typical for sandy aquifers, the annual risk prediction is 100 %.

5. Results and discussion

5.1. Sensitivity analysis limitations in nonlinear problems

For the sensitivity analysis performed in this study, we allowed a relatively straightforward form in that the selected output—the health risk—is a unique and well-identified quantitative function. This output permitted the simple calculation of sensitivity as the log ratio between changes in the value of each input factor and the induced changes in the value of this unique output function. However, our approach is somewhat limited, and our results may be regarded as nonuniversal, as they do not account for the interdependence of the influences of input parameters. This is typical of nonlinear problems and leads to only partial sensitivities. For example, we observe that the effect of the immobile virus inactivation coefficient on the viral peak reduction (and the health risk) is enhanced by a high K_{att}/K_{det}. This enhancement occurs as high attachment rates combine with low detachment rates to produce sustained high concentrations of immobile viruses and hence high rates of immobile virus inactivation, which enhances the effect of this mechanism on the overall virus-reduction dynamics. Similarly, the K_{att} sensitivity markedly increases with K_{det} as illustrated in Fig. 12. The partial sensitivities calculated in such cases are taken as the maximum sensitivities. In contrast, the sensitivity of the hydrodynamic input parameter v_D is fairly invariable in regard to the reaction input parameters. Finally, the internal variability of sensitivities obtained for each parameter because of changes to another parameter are smaller than the overall differences between the sensitivities of distinct parameters (external variability) in such a manner that the obtained hierarchal importance of parameters influences is an unaltered, robust result.

5.2. Uncertainty of kinetic reaction coefficients

We demonstrate that the current state of knowledge related to virus reaction coefficients limits our ability to produce robust predictions of virus-related health risks. Indeed, our models show that the variability in these coefficients (compiled from published experimental values) induces an extreme variability of viral peak penetration into aquifers (1–60 m) and reduction (1–15 log) and variability in the annual health risk at 30 m from virtually zero to 100 %. The mobile virus inactivation coefficient in groundwater can be measured directly from batch tests; however, estimates for the three other mechanisms, namely, attachment, detachment and immobile virus inactivation, are much more complex, as they require applying an inverse method to temporal and spatial series for experimental data obtained either from continuous-flow sand columns or field tests. Such an approach permits measuring the complete set of four coefficients, which is, to our knowledge, currently available in only three studies. Consequently, a massive

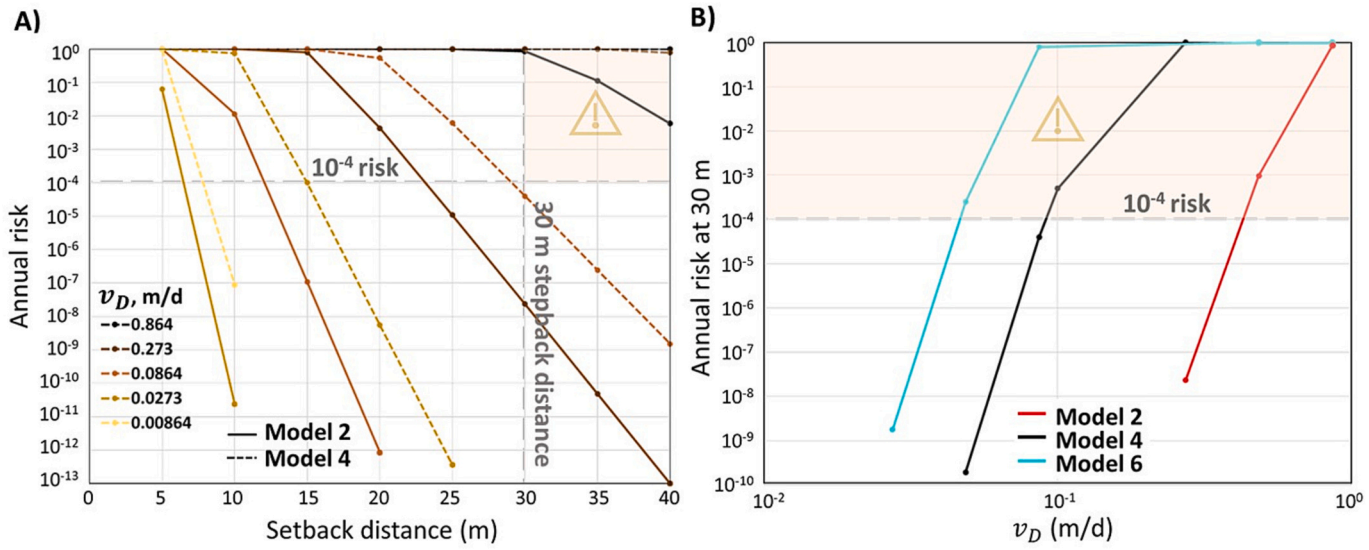


Fig. 13. Simulation results for the influence of Darcy velocity v_D on the annual health risk predictions for selected values of kinetic reaction coefficients (see Table 1). A) Risk as a function of setback distances for various values of v_D (variations by a factor 0.5 log); B) risk at 30 m setback distance as a function of v_D. The simulation parameters are $\alpha = 2$ m and $\theta = 0.3$. The shaded area with a warning symbol corresponds to a health risk exceeding the 10^{-4} threshold, i.e., danger zone.

disparity exists between the state of knowledge for mobile virus inactivation and the three other coefficients. Moreover, numerous studies quantifying the mobile virus inactivation coefficient have submitted conclusive remarks on its variability and the influence of groundwater physicochemical properties. Such variability in natural environments may also be expected for the other three mechanisms, albeit it is unknown. Finally, significant methodological differences exist among the published experimental studies (Fig. 7). Improving our experimental knowledge of the viral kinetic reaction coefficients is a cornerstone for modeling the fate of viruses in aquifers.

The lack of quantitative constraints on the correlative relationships between the four reaction coefficients limits model calibration. When scanning the full range of experimental variability, some configurations may be unrealistic because of the physical links between the mechanisms. Additional experiment-based constraints of the four sets of coefficients are required to reduce this knowledge gap and uncertainty in the risk predictions.

Our models show that, as a general rule, the long-term reduction in viral concentrations is determined mainly by immobile virus inactivation and, to a lower degree, by detachment. These are known as *immobile phase parameters* in that their rates are first-order functions of the immobile virus concentration (Eq. 6). The persistence of residual virus concentrations, which has been reported from field measurements (Blanford et al., 1995), is governed by these immobile phase parameters and is illustrated by the immobile inactivation coefficient determining the slope of the characteristic long trails of virus breakthrough curves (Fig. 3). As explained above, long-term residual virus concentrations (despite their low values) can affect the annual risk in a non-negligible fashion because risk is cumulative over time (eqs. 8 and 9). Here again, improving our understanding of these two immobile phase parameters is necessary for sound health risk assessment.

5.3. Influence of the source concentration

In this study, we held virus concentrations at the source of the models at $C_0 = 9.2$ log/L $= 1.5 \times 10^9$ viruses/L. The concentration range estimated from calculations based on rotavirus concentrations in feces and their removal from septic systems is 4.9–0.9 log/L or 7.9×10^4 to 7.9×10^9 viruses/L. These estimates match well the 3 to 10.9 log/L concentrations measured from clarified wastewater in septic effluent (Charles et al., 2003). We investigated the implications of the fixed C_0 value on the models by quantifying the risk sensitivity to C_0. Expectedly, this led to a unit sensitivity value, that is, 1-log variation in C_0 induces 1-log variation in the risk prediction, all parameters being equal; a very low value relative to sensitivities >20 was obtained for other input parameters. This suggests that C_0 is not a significant source of uncertainty in the models.

5.4. Unassessed hydrogeological and environmental parameters

Highly conductive flow media, such as fractured rocks, karst, sand–gravel aquifers, and steep hydraulic gradients typical of hilly landscapes are prone to the extensive penetration of viral pulses (Schijven and Hassanizadeh, 2000; Bhattacharjee et al., 2002; Hlavinek et al., 2008; Masciopinto et al., 2008). More specifically, the issue of viral pulse reactive transport into fractured hard rock is complex because of the combination of extremely rapid pulse penetration and sustained viral concentrations associated with the delayed transfer between *internal blocks* and the drained fault or fracture. Internal blocks refer here to low-conductivity, high-storage-capacity rock mass blocks separated by the major fracture drains, which are in contrast, high-conductivity, low-storage tabular flow domains that follow a typical conceptual model for fractured media. On the one hand, very rapid pore velocities in fracture and fault drains have been reported from field investigations (Novakowski et al., 2006): between 6 and 22 m/d (median 11 m/d, 8 measurements) in fracture pathways isolated with packers (undisturbed hydraulic gradient) and between 2 and 388 m/d (median 55 m/d, 13 measurements) in non-isolated rock mass fracture networks. These values agree with the compilation produced by Worthington et al. (2016) of 49 sink-to-spring tracer experiments in siliceous hard rock aquifers and a median 170 m/d.

Given the marked sensitivity of risk to flow velocity predicted from our models, one can anticipate a very high risk level in fractured hard rock aquifers; this corroborates the epidemiological observations that identify these domains as being particularly vulnerable to contamination and health risks (e.g., Allen et al., 2017). This may be accentuated by delayed release effects between blocks and drains caused by their strongly contrasting conductive and storage properties. Such two-speed responses are well known for pressure transfers (double porosity models); they are expected to also operate on mass transfers, leading to persistent viral concentrations in the aquifer. Beyond these qualitative statements, modeling the fate of viruses within fractured hard rock

remains poorly known and must be the focus of future studies.

Conversely, some hydrogeological components are known (qualitatively) to act as barriers to viral propagation. The most effective barrier is the unsaturated zone because of the retention of viruses at the water–air interface (Bradford and Torkzaban, 2008) and the low pore velocity (low relative conductivity). This effect is not accounted for in our models, which conceptually consider the water table as being at the bottom of the seepage field. In most actual contexts—where an unsaturated zone lies deeper—our risk predictions based only on saturated transport will be significantly limited. The quantification of this reduction requires further investigation.

Finally, epidemiologic studies note that rain events significantly influence viral occurrences in the subsurface (Bradbury et al., 2013; Hynds et al., 2014; Allen et al., 2017); however, our understanding of such a causal relationship remains qualitative. We do not account for this effect in our modeling, although this phenomenon would be expected to significantly affect mass transfers of viruses in the unsaturated zone.

6. Conclusion

Our reactive viral transport model can serve as a new tool and has produced insights into the transport of viruses within aquifers. Frohnert et al. (2014) first implemented a fully kinetic model using the HYDRUS 1D code, and these authors applied their model to reproduce and interpret their own experimental observations of virus transport in saturated columns. Their model was not validated by other experimental data, such as that from in situ tests conducted by Schijven et al. (1999). Our new model developed with the FEFLOW code is a novel approach that contributes to establishing a more comprehensive model validated by laboratory and field experimental results. Furthermore, this new model can predict the risk of groundwater viral contamination and has demonstrated its utility as a powerful tool for performing prognostic investigations and sensitivity analyses. Prognostic exploitation of the model was designed to explore the dynamics of penetration and the persistence of virus pulses into aquifers. It exposes the complexity of viral reduction, where four kinetic reactions exert interdependent effects. Residual virus concentrations in groundwater occur due to transport slow-down, favoured by attachment and detachment contrasted kinetics and a low immobile viruses inactivation rate. The sensitivity analysis of the transport model to hydrogeologic and biochemical input parameters shows that the hydraulic conductivity, the virus attachment rate and the immobile virus inactivation rate are first-order parameters exerting the most prominent influence on virus persistence in aquifers. Concomitantly, the virus concentration time and space series obtained from transport modeling are used to predict the annual health risk for water consumers within neighbourhood, into rural residential contexts supplied by individual private wells and following standard dose-response relationships. Such comprehensive methodology where reactive transport modeling is implemented with risk evaluation is original. It allows linking quantitatively the annual risk to the setback distances in regards to benchmark regulatory values. An important result is that within the range of values provided by the current state of knowledge on virus kinetic coefficients, the 30 m regulatory setback distance is critical into many real conditions where aquifers are conductive. Further in-situ experimental studies are required to improve constrains on virus kinetics, specifically the immobile virus inactivation and detachment rates which estimations exhibit obvious discrepancies due to methodological bias (in-situ vs. sand column), while they exert a deep influence on the fate of virus.

CRediT authorship contribution statement

Silvain Rafini: Writing- Original draft preparation. Conceptualization, Methodology, Software, validation, Investigation, Formal analysis.

Romain Chesnaux: Supervision, Project administration, Funding acquisition, Writing, Methodology, Reviewing and Editing.

Kim Maren Lompe: Investigation, writing, Methodology, Reviewing and Editing.

Benoit Barbeau: Supervision, Writing, Methodology, Reviewing and Editing.

Dominique Claveau-Mallet: Supervision, Writing, Methodology, Reviewing and Editing.

Dominique Richard: Reviewing and Editing.

Declaration of competing interest

Silvain Rafini reports financial support was provided by Quebec ministry of evironment.

Data availability

The authors do not have permission to share data.

Acknowledgments

The authors acknowledge the financial support of Ministère du Développement Durable, de l'Environnement et de la Lutte contre les changements climatiques of the province of Quebec, Canada.

References

Adegoke, A.A., Stenstrom, T.A., 2019. Septic systems. In: Rose, J.B., Jiménez-Cisneros, B. (Eds.), Water and Sanitation for the 21st Century: Health and Microbiological Aspects of Excreta and Wastewater Management (Global Water Pathogen Project). Part 4: Management of Risk from Excreta and Wastewater - section: Sanitation system technologies, pathogen reduction in non-sewered (on-site) system technologies. Michigan State University. https://doi.org/10.14321/waterpathogens.59.

Allen, A.S., Borchardt, M.A., Kieke, B.A., Dunfield, K.E., Parker, B.L., 2017. Virus occurrence in private and public wells in a fractured dolostone aquifer in Canada. Hydrogeol. J. 25 (4), 1117–1136. https://doi.org/10.1007/s10040-017-1557-5.

Anders, R., Chrysikopoulos, C.V., 2009. Transport of viruses through saturated and unsaturated columns packed with sand. Transp. Porous Media 76 (1), 121–138.

Anderson, E.J., Weber, S.G., 2004. Rotavirus infection in adults. Lancet Infect. Dis. 4 (2), 91–99. https://doi.org/10.1016/S1473-3099(04)00928-4.

Azadpour-Keeley, A., Ward, C.H., 2005. Transport and survival of viruses in the subsurface—processes, experiments, and simulation models. Remediat. J. 15 (3), 23–49. https://doi.org/10.1002/rem.20048.

Azadpour-Keeley, A., Faulkner, B.P., Chen, J., 2003. Movement and Longevity of Viruses in the Subsurface. Environmental Protection Agency, National Risk Management Research Laboratory, Washington, DC.

Bales, R.C., Li, S., Maguire, K.M., Yahya, M.T., Gerba, C.P., 1993. MS-2 and poliovirus transport in porous media: hydrophobic effects and chemical perturbations. Water Resour. Res. 29 (4), 957–963. https://doi.org/10.1029/92WR02986.

Bales, R.C., Li, S., Maguire, K.M., Yahya, M.T., Gerba, C.P., Harvey, R.W., 1995. Virus and bacteria transport in a sandy aquifer, Cape Cod, MA. Ground Water 33 (4), 653–661. https://doi.org/10.1111/j.1745-6584.1995.tb00321.x.

Barber, N.L., 2009. Summary of estimated water use in the United States in 2005. U.S. Geological Survey fact sheet 2009–3098. US Department of the Interior, US Geological Survey, Reston, VA.

Bennett, A., Pollock, L., Jere, K.C., Pitzer, V.E., Lopman, B., Bar-Zeev, N., Iturriza-Gomara, M., Cunliffe, N.A., 2020. Duration and density of fecal rotavirus shedding in vaccinated Malawian children with rotavirus gastroenteritis. J. Infect. Dis. 222 (12), 2035–2040. https://doi.org/10.1093/infdis/jiz612.

Betancourt, W.Q., Schijven, J., Regnery, J., Wing, A., Morrison, C.M., Drewes, J.E., Gerba, C.P., 2019. Variable nonlinear removal of viruses during transport through a saturated soil column. J. Contam. Hydrol. 223, 103479 https://doi.org/10.1016/j.jconhyd.2019.04.002.

Bhattacharjee, S., Ryan, J.N., Elimelech, M., 2002. Virus transport in physically and geochemically heterogeneous subsurface porous media. J. Contam. Hydrol. 57 (3–4), 161–187. https://doi.org/10.1016/S0169-7722(02)00007-4.

Bitton, G., Marshall, K.C., 1980. Adsorption of Microorganisms to Surfaces. John Wiley & Sons, Inc. https://doi.org/10.1097/00010694-198011000-00012

Blanc, R., Nasser, A., 1996. Effect of effluent quality and temperature on the persistence of viruses in soil. Water Sci. Technol. 33 (10−11), 237–242. https://doi.org/10.2166/wst.1996.0680.

Blanford, W.J., Brusseau, M.L., Jim Yeh, T.C., Gerba, C.P., Harvey, R., 2005. Influence of water chemistry and travel distance on bacteriophage PRD-1 transport in a sandy aquifer. Water Res. 39 (11), 2345–2357. https://doi.org/10.1016/j.watres.2005.04.009.

Blaschke, A.P., Derx, J., Zessner, M., Kirnbauer, R., Kavka, G., Strelec, H., Farnleitner, A. H., Pang, L., 2016. Setback distances between small biological wastewater treatment systems and drinking water wells against virus contamination in alluvial aquifers. Sci. Total Environ. 573, 278–289. https://doi.org/10.1016/d.scitotenv.2016.08.075.

Borchardt, M.A., Bertz, P.D., Spencer, S.K., Battigelli, D.A., 2003. Incidence of enteric viruses in groundwater from household wells in Wisconsin. Appl. Environ. Microbiol. 69 (2), 1172–1180. https://doi.org/10.1128/AEM.69.2.1172-1180.2003.

Borchardt, M.A., Spencer, S.K., Kieke, B.A., Lambertini, E., Loge, F.J., 2012. Viruses in nondisinfected drinking water from municipal wells and community incidence of acute gastrointestinal illness. Environ. Health Perspect. 120 (9), 1272–1279. https://doi.org/10.1289/ehp.1104499.

Bradbury, K.R., Borchardt, M.A., Gotkowitz, M., Spencer, S.K., Zhu, J., Hunt, R.J., 2013. Source and transport of human enteric viruses in deep municipal water supply wells. Environ. Sci. Technol. 47 (9), 4096–4103. https://doi.org/10.1021/es400509b.

Bradford, S.A., Torkzaban, S., 2008. Colloid transport and retention in unsaturated porous media: a review of interface-, collector-, and pore-scale processes and models. Vadose Zone J. 7, 667–681. https://doi.org/10.2136/vzj2007.0092.

Bremer, J.E., Harter, T., 2012. Domestic wells have high probability of pumping septic tank leachate. Hydrol. Earth Syst. Sci. 16 (8), 2453–2467. https://doi.org/10.5194/hess-16-2453-2012.

Charles, K., Ashbolt, N., Ferguson, C., Roser, D., McGuinness, R., Deere, D., 2003. Centralised versus decentralised sewage systems: a comparison of pathogen and nutrient loads released into Sydney's drinking water catchments. Water Sci. Technol. 48 (11−12), 53–60. https://doi.org/10.2166/wst.2004.0802.

Chrysikopoulos, C.V., Katzourakis, V.E., 2015. Colloid particle size-dependent dispersivity. Water Resour. Res. 51 (6), 4668–4683.

Chrysikopoulos, C.V., Sim, Y., 1996. One-dimensional virus transport in homogeneous porous media with time-dependent distribution coefficient. J. Hydrol. 185 (1–4), 199–219.

Diersch, HJ. G. (2014) Flow in saturated porous media: groundwater flow. In: FEFLOW. Springer, Berlin, Heidelberg. doi:https://doi.org/10.1007/978-3-642-38739-5_9.

Doherty, J., 2015. Calibration and Uncertainty Analysis for Complex Environmental Models. Watermark Numerical Computing.

Doherty, J., 2018. Model-Independent Parameter Estimation User Manual, Part I: PEST, SENSAN and Global Optimisers, Seventh ed. Watermark Numerical Computing.

Dullemont, Y.J., Schijven, J., Hijnen, W., Colin, M., Knezev, A., Oorthuizen, W., 2006. Removal of microorganisms by slow sand filtration. In: Nakamoto, N., Graham, N., Collins, M.R., Gimbel, R. (Eds.), Progress in Slow Sand and Alternative Biofiltration Processes. IWA Publishing, pp. 12–20. https://doi.org/10.2166/9781780406381.

Eregno, F.E., Heistad, A., 2019. On-site treated wastewater disposal systems - the role of stratified filter medias for reducing the risk of pollution. Environ. Int. 124, 302–311. https://doi.org/10.1016/j.envint.2019.01.008.

Féret, A., 2016. La qualité de l'eau des puits individuels au Québec: comment améliorer les pratiques d'analyses? Master's, Université de Sherbrooke, Sherbrooke, QC, Canada. https://savoirs.usherbrooke.ca/handle/11143/8193.

Ferroud, A., Rafini, S., Chesnaux, R., 2019. Using flow dimension sequences to interpret nonuniform aquifers with constant-rate pumping-tests: a review. J. Hydrol. X 2, 100003. https://doi.org/10.1016/j.hydroa.2018.100003.

Frohnert, A., Apelt, S., Klitzke, S., Chorus, I., Szewzyk, R., Selinka, H.C., 2014. Transport and removal of viruses in saturated sand columns under oxic and anoxic conditions—potential implications for groundwater protection. Int. J. Hyg. Environ. Health 217 (8), 861–870. https://doi.org/10.1016/j.ijheh.2014.06.004.

Gerba, C.P., Smith, J.E., 2005. Sources of pathogenic microorganisms and their fate during land application of wastes. J. Environ. Qual. 34 (1), 42–48.

Grant, R.F., Juma, N.G., McGill, W.B., 1993. Simulation of carbon and nitrogen transformations in soil: microbial biomass and metabolic products. Soil Biol. Biochem. 25 (10), 1331–1338. https://doi.org/10.1016/0038-0717(93)90047-F.

Gunnarsdottir, M.J., Gardarsson, S.M., Andradottir, H.O., 2013. Microbial contamination in groundwater supply in a cold climate and coarse soil: case study of norovirus outbreak at Lake Mývatn, Iceland. Nord. Hydrol. 44 (6), 1114–1128. https://doi.org/10.2166/nh.2013.076.

Health Canada, 2019. Guidelines for Canadian drinking water quality: guideline technical document — enteric viruses. Catalogue no. H129-6/2019E-PDF. Water and Air Quality Bureau, Healthy Environments and Consumer Safety Branch, Health Canada, Ottawa, Ontario.

Hijnen, W.A.M., Baars, E., Bosklopper, T.G.J., Van Der Veer, A.J., Meijers, R.T., Medema, G.J., 2004. Influence of DOC on the inactivation efficiency of ozonation assessed with *Clostridium perfringens* and a lab-scale continuous flow system. Ozone Sci. Eng. 26 (5), 465–473. https://doi.org/10.1080/01919510490507784.

Hiscock, K.M., 2011. Groundwater in the 21st century – meeting the challenges. In: Jones, J.A.A. (Ed.), Sustaining Groundwater Resources: A Critical Element in the Global Water Crisis. Springer, Netherlands, pp. 207–225. https://doi.org/10.1007/978-90-481-3426-7_13.

Hlavinek, P., Bonacci, O., Mahrikova, I., Marsalek, J. (Eds.), 2008. Dangerous Pollutants (Xenobiotics) in Urban Water Cycle. Springer. https://doi.org/10.1007/978-1-4020-6795-2.

Hurst, C.J., Gerba, C.P., Cech, I., 1980. Effects of environmental variables and soil characteristics on virus survival in soil. Appl. Environ. Microbiol. 40 (6), 1067–1079. https://doi.org/10.1128/aem.40.6.1067-1079.1980.

Hynds, P.D., Thomas, M.K., Pintar, K.D.M., 2014. Contamination of groundwater systems in the US and Canada by enteric pathogens, 1990–2013: a review and pooled-analysis. PLoS One 9 (5), e93301. https://doi.org/10.1371/journal.pone.0093301.

Jin, Y., Flury, M., 2002. Fate and transport of viruses in porous media. Adv. Agron. 77, 39–102. https://doi.org/10.1016/S0065-2113(02)77013-2.

Jin, H., Leser, G.P., Zhang, J., Lamb, R.A., 1997. Influenza virus hemagglutinin and neuraminidase cytoplasmic tails control particle shape. EMBO J. 16 (6), 1236–1247. https://doi.org/10.1093/emboj/16.6.1236.

Keswick, B.H., Gerba, C.P., Secor, S.L., Cech, I., 1982. Survival of enteric viruses and indicator bacteria in groundwater. J. Environ. Sci. Health. A Environ. Sci. Eng. 17 (6), 903–912. https://doi.org/10.1080/10934528209375085.

Khare, D., Jat, M.K., Mishra, P.K., 2017. Groundwater hydrology: An overview. In: Srinivasa Raju, K., Vasan, A. (Eds.), Sustainable Holistic Water Resources Management in a Changing Climate. Jain Brothers, pp. 4.1–4.26.

Lindstrom, F.T., 1976. Pulsed dispersion of trace chemical concentrations in a saturated sorbing porous medium. Water Resour. Res. 12 (2), 229–238.

Lusk, M.G., Toor, G.S., Yang, Y.Y., Mechtensimer, S., De, M., Obreza, T.A., 2017. A review of the fate and transport of nitrogen, phosphorus, pathogens, and trace organic chemicals in septic systems. Crit. Rev. Environ. Sci. Technol. 47 (7), 455–541. https://doi.org/10.1080/10643389.2017.1327787.

Macías, J.A., Vargas, E.A., Sracek, O., 2017. A comparative analysis of two methodologies to estimate well protection zones for transport of viruses from septic tanks in volcanic aquifers in Costa Rica. Environ. Earth Sci. 76 (6), 244. https://doi.org/10.1007/s12665-017-6563-3.

Masciopinto, C., La Mantia, R., Chrysikopoulos, C.V., 2008. Fate and transport of pathogens in a fractured aquifer in the Salento area, Italy. Water Resour. Res. 44 (1), 1–18.

Ministère de l''Environnement, d. l. L. c. l. c. c., de la Faune et des Parcs (MELCC), 2023. Eaux souterraines. Ministère de l'Environnement, de la Lutte contre les changements climatiques, de la Faune et des Parcs, Gouvernement du Québec. https://www.environnement.gouv.qc.ca/eau/souterraines/index.htm. https://doi.org/10.1029/2006WR005643.

Moore, R.S., Taylor, D.H., Sturman, L.S., Reddy, M.M., Fuhs, G.W., 1981. Poliovirus adsorption by 34 minerals and soils. Appl. Environ. Microbiol. 42 (6), 963–975.

Murphy, H.M., Thomas, M.K., Medeiros, D.T., McFadyen, S., Pintar, K.D.M., 2016. Estimating the number of cases of acute gastrointestinal illness (AGI) associated with Canadian municipal drinking water systems. Epidemiol. Infect. 144 (7), 1371–1385. https://doi.org/10.1017/S0950268815002083.

Murphy, H.M., Prioleau, M.D., Borchardt, M.A., Hynds, P.D., 2017. Epidemiological evidence of groundwater contribution to global enteric disease, 1948-2015. Hydrogeol. J. 25 (4), 981–1001. https://doi.org/10.1007/s10040-017-1543-y.

Nasser, A.M., Oman, S.D., 1999. Quantitative assessment of the inactivation of pathogenic and indicator viruses in natural water sources. Water Res. 33 (7), 1748–1752. https://doi.org/10.1016/S0043-1354(98)00380-7.

Nasser, A.M., Tchorch, Y., Fattal, B., 1993. Comparative survival of E. Coli, F bacteriophages, HAV and poliovirus 1 in wastewater and groundwater. Water Sci. Technol. 27 (3–4), 401–407. https://doi.org/10.2166/wst.1993.0381.

Nkedi-Kizza, P., Shinde, D., Savabi, M.R., Ouyang, Y., Nieves, L., 2006. Sorption kinetics and equilibria of organic pesticides in carbonatic soils from South Florida. J. Environ. Qual. 35 (1), 268–276.

Novakowski, K., Bickerton, G., Lapcevic, P., Voralek, J., Ross, N., 2006. Measurements of groundwater velocity in discrete rock fractures. J. Contam. Hydrol. 82 (1–2), 44–60. https://doi.org/10.1016/j.jconhyd.2005.09.001.

O'Brien, R.T., Newman, J.S., 1977. Inactivation of polioviruses and coxsackieviruses in surface water. Appl. Environ. Microbiol. 33 (2), 334–340. https://doi.org/10.1128/aem.33.2.334-340.1977.

Ogata, A., Banks, R.B., 1961. A Solution of the Differential Equation of Longitudinal Dispersion in Porous Media: Fluid Movement in Earth Materials. US Government Printing Office.

Pang, L., 2009. Microbial removal rates in subsurface media estimated from published studies of field experiments and large intact soil cores. J. Environ. Qual. 38, 1531–1559. https://doi.org/10.2134/jeq2008.0379.

Powell, K.L., Taylor, R.G., Cronin, A.A., Barrett, M.H., Pedley, S., Sellwood, J., Trowsdale, S.A., Lerner, D.N., 2003. Microbial contamination of two urban sandstone aquifers in the UK. Water Res. 37 (2), 339–352. https://doi.org/10.1016/S0043-1354(02)00280-4.

Powelson, D.K., Simpson, J.R., Gerba, C.P., 1991. Effects of organic matter on virus transport in unsaturated flow. Appl. Environ. Microbiol. 57 (8), 2192–2196. https://doi.org/10.1128/aem.57.8.2192-2196.1991.

Rao, P.S.C., Davidson, J.M., Jessup, R.E., Selim, H.M., 1979. Evaluation of conceptual models for describing nonequilibrium adsorption-desorption of pesticides during steady-flow in soils. Soil Sci. Soc. Am. J. 43 (1), 22–28. https://doi.org/10.2136/sssaj1979.03615995004300010004x.

Ratha, D.N., Hari Prasad, K.S., Ojha, C.S., 2009. Analysis of virus transport in groundwater and identification of transport parameters. Pract. Period. Hazard. Toxic Radioact. Waste Manag. 13 (2), 98–109. https://doi.org/10.1061/(ASCE)1090-025X(2009)13:2(98).

Reynolds, K.A., Mena, K.D., Gerba, C.P., 2008. Risk of waterborne illness via drinking water in the United States. Rev. Environ. Contam. Toxicol. 192, 117–158.

Schijven, J.F., Hassanizadeh, S.M., 2000. Removal of viruses by soil passage: overview of modeling, processes, and parameters. Crit. Rev. Environ. Sci. Technol. 30 (1), 49–127. https://doi.org/10.1080/10643380091184174.

Schijven, J.F., Hoogenboezem, W., Hassanizadeh, M., Peters, J.H., 1999. Modeling removal of bacteriophages MS2 and PRD1 by dune recharge at Castricum, Netherlands. Water Resour. Res. 35 (4), 1101–1111. https://doi.org/10.1029/1998WR900108.

Schijven, J.F., Hassanizadeh, S.M., de Bruin, H.A.M., 2002. Column experiments to study nonlinear removal of bacteriophages by passage through saturated dune sand. J. Contam. Hydrol. 58 (3–4), 243–259. https://doi.org/10.1016/S0169-7722(02)00040-2.

Schulze-Makuch, D., 2005. Longitudinal dispersivity data and implications for scaling behavior. Ground Water 43 (3), 443–456. https://doi.org/10.1111/j.1745-6584.2005.0051.x.

Schuster, C.J., Ellis, A.G., Robertson, W.J., Charron, D.F., Aramini, J.J., Marshall, B.J., Medeiros, D.T., 2005. Infectious disease outbreaks related to drinking water in Canada, 1974-2001. Can. J. Public Health 96 (4), 254–258. https://doi.org/10.1007/BF03405157.

Sim, Y., Chrysikopoulos, C.V., 1996. One-dimensional virus transport in porous media with time-dependent inactivation rate coefficients. Water Resour. Res. 32 (8), 2607–2611. https://doi.org/10.1029/96wr01496.

Smith, A., Reacher, M., Smerdon, W., Adak, G.K., Nichols, G., Chalmers, R.M., 2006. Outbreaks of waterborne infectious intestinal disease in England and Wales, 1992-2003. Epidemiol. Infect. 134, 1141–1149. https://doi.org/10.1017/S0950268806006406.

Sobsey, M.D., Battigelli, D.A., Handzel, T.R., Schwab, K.J., 1995. Male-Specific, Coliphages as Indicators of Viral Contamination of Drinking Water. American Water Works Association Research Foundation.

Toride, N., Leij, F.J., Van Genuchten, M.T., 1995. The CXTFIT Code for Estimating Transport Parameters from Laboratory or Filed Tracer Experiments. US Salinity Laboratory.

Torkzaban, S., Hassanizadeh, S.M., Schijven, J.F., Van Den Berg, H.H.J.L., 2006. Role of air-water interfaces on retention of viruses under unsaturated conditions. Water Resour. Res. 42 (12), W12S14. https://doi.org/10.1029/2006WR004904.

Trimper, S. A. (2010). *The presence and transport of human enteric viruses in fractured bedrock aquifers. (M.Sc.)*. Queen's University. https://qspace.library.queensu.ca/handle/1974/6199.

Tufenkji, N., 2007. Modeling microbial transport in porous media: traditional approaches and recent developments. Adv. Water Resour. 30 (6–7), 1455–1469. https://doi.org/10.1016/j.advwatres.2006.05.014.

United States Environmental Protection Agency (USEPA), 2022. Private drinking water wells. United States Environmental Protection Agency (USEPA), US Government. https://www.epa.gov/privatewells.

van der Wielen, P.W.J.J., Blokker, M., Medema, G.J., 2006. Modelling the length of microbiological protection zones around phreatic sandy aquifers in the Netherlands. Water Sci. Technol. 54 (3), 63–69. https://doi.org/10.2166/wst.2006.449.

van der Wielen, P.W.J.J., Senden, W.J.M.K., Medema, G., 2008. Removal of bacteriophages MS2 and phiX174 during transport in a sandy anoxic aquifer. Environ. Sci. Technol. 42 (12), 4589–4594. https://doi.org/10.1021/es800156c.

Worthington, S.R., Davies, G.J., Alexander, E.C., 2016. Enhancement of bedrock permeability by weathering. Earth Sci. Rev. 160, 188–202. https://doi.org/10.1016/j.earscirev.2016.07.002.

Yates, M.V., Gerba, C.P., Kelley, L.M., 1985. Virus persistence in groundwater. Appl. Environ. Microbiol. 49 (4), 778–781. https://doi.org/10.1128/aem.49.4.778-781.1985.